Physics Opportunities at Neutrino Factories *

J.J. Gomez-Cadenas[1], *D.A. Harris*[2]

[1]Department of Atomic and Nuclear Physics and IFIC, University of Valencia, Spain; e-mail: *gomez@ific.uv.es*; [2] Fermilab, Batavia,Illinois, USA; e-mail: *dharris@fnal.gov*

KEYWORDS: neutrino oscillations, solar neutrinos, atmospheric neutrinos, leptonic CP violation, muon storage ring

ABSTRACT:

This article describes the physics capabilities of a future facility which would be capable of providing extremely intense and clean neutrino beams. This facility, called a *neutrino factory*, consists of a muon storage ring with long straight sections, pointed at experimental areas both near and far. Given the expected intensity of muons stored in the rings, this facility could provide to the lepton sector what decades of precision kaon and B experiments have provided to the quark sector. One would measure with unprecedented precision the parameters of the leptonic mixing matrix, explore the neutrino mass pattern and, ultimately, search for CP violation in the leptonic sector. In addition, the high fluxes at a neutrino factory would open up a whole new field in precision neutrino scattering physics close to the ring itself.

CONTENTS

*This article is dedicated to the past and future successes of our colleagues at Super-Kamiokande

1 INTRODUCTION

The idea of creating a beam of muons and placing it in a storage ring with straight sections which would then create neutrino beams can be found as early as 1962. One proposal by Tinlot and Green involved creating muons from electron beams at SLAC (1). Later ideas by Collins, Wojicki (2), and Koskarev (3) involved creating focused beams of pions and collecting them in a storage ring, where they would quickly decay into muon beams. The straight sections in the storage rings would point to experimental areas, which would then be illuminated by the intense neutrino beams created by the decays of the circulating muons.

Also around this time, Davis *et al* had started their historical experiment in the Homestake mine (4), first to find evidence for and later to measure the flux of neutrinos coming from the sun. This experiment ultimately measured about half the predicted (5) ν_e rate. The disagreement was called, variously, the "solar neutrino anomaly" and "solar neutrino problem", names that suggest the mood of the times. It was thought that something was wrong with the experiment, the theory, or both.

The Davis experiment has been operating since 1964 (6) and five other experiments have joined in, GALLEX (7), SAGE (8) Kamiokande and Super-Kamiokande (9) and most recently Sudbury Neutrino Observatory (SNO) (10). All of them have found fewer electron neutrinos than predicted by the Standard Solar Model (SSM) (5).

During the 1980s, another anomaly appeared, this one in the rates of neutrinos produced in the atmosphere. These fluxes, as measured by several underground experiments (11) were also smaller than theoretical expectations. In particular, while the observed flux of atmospheric ν_e's was roughly consistent with the

theoretical models, the flux of ν_μ's was only about half the prediction.

In 1998, at the XVIIIrd International Conference on Neutrino Physics and Astrophysics held in Takayama, Japan, the Super-Kamiokande collaboration reported the first compelling experimental evidence (12) that the "atmospheric neutrino problem" could be explained in terms of a theoretical idea even older than the Davis experiment, the brain child of Pontecorvo, who, in 1957, suggested the possibility that there could be oscillations between the different neutrino flavors (13), a notion further developed by Maki, Nakagawa, and Sakata (14).

Also in 1998, Geer (15) reinvented the neutrino factory idea, demonstrating that, a) collecting, accelerating and storing muons in the energy range of tens of GeV was feasible with the existing expertise at Fermilab and other laboratories (18), and b) that the clean neutrino beams arising from muon decays would be uniquely suited for neutrino oscillation experiments.

There remains one more "anomaly" in this history: in 1995 the Liquid Scintillator Neutrino Detector (LSND) collaboration observed a significant excess over background of $\bar{\nu}_e$'s in an almost pure $\bar{\nu}_\mu$ beam made from a beam created from pion decays at Los Alamos (16). Because they observed the appearance of a new flavor of neutrinos produced in a accelerator-based beam and not disappearance from an external source, it was interpreted as neutrino oscillations, although they could not be simply another manifestation of either the solar or the atmospheric signatures. The KARMEN experiment at the Rutherford Appleton Laboratory probes a similar region of parameter space, and has ruled out parts of but not all of the allowed parameter space from the LSND result (17). The implications of this signature being confirmed as oscillations are enormous, as we will discuss shortly.

Before describing what a neutrino factory can bring to this diverse field, it is important to understand how oscillation measurements are made in the first place. Since neutrinos are weakly interacting particles, the can only be detected when they exchange a $W^{\pm}$ or a Z with particles (electrons or quarks) in a detector. If a Z is exchanged (called a "neutral current" interaction) the outgoing lepton is still a neutrino, and one cannot distinguish the flavor of the interacting neutrino. However, if a $W^{\pm}$ is exchanged, as in the top four diagrams in Figure 1, a charged lepton leaves the interaction. The most straightforward way to measure neutrino oscillations is to use a detector which can identify the flavor of the outgoing lepton, assuming the flavor of the incoming neutrino is known.

To understand why neutrino factories are so well-suited to oscillation measurements it is worthwhile to compare muon-induced and conventional neutrino beams. The latter are made by hitting a target with an intense proton beam, focusing the resulting hadrons, and letting them decay in a long tunnel. By focusing only one charge of hadrons, the produced beam can be an "almost" 100 % pure ν_μ or $\bar{\nu}_\mu$ beam.

However, that "almost" is what makes oscillation experiments difficult. There is a small contamination, of the order of 1 % of ν_e and antineutrinos of both flavors, produced by the three-body decays $K^+ \to e^+\pi^0\nu_e$, $K_L \to e^{\pm}\pi^{\mp}\nu_e(\bar{\nu}_e)$, and tertiary muons that decay before they can be absorbed. The neutrino backgrounds in antineutrino beams can be even more severe, since the neutrino cross section is twice that of the antineutrino cross section. As an example, Fig. 2(left), shows the neutrino beam produced by the SPS machine at CERN, which illuminated the NOMAD (19) and CHORUS (20) experiments. Notice that although it is mostly a ν_μ beam, a total of four out of the six possible neutrino flavors are

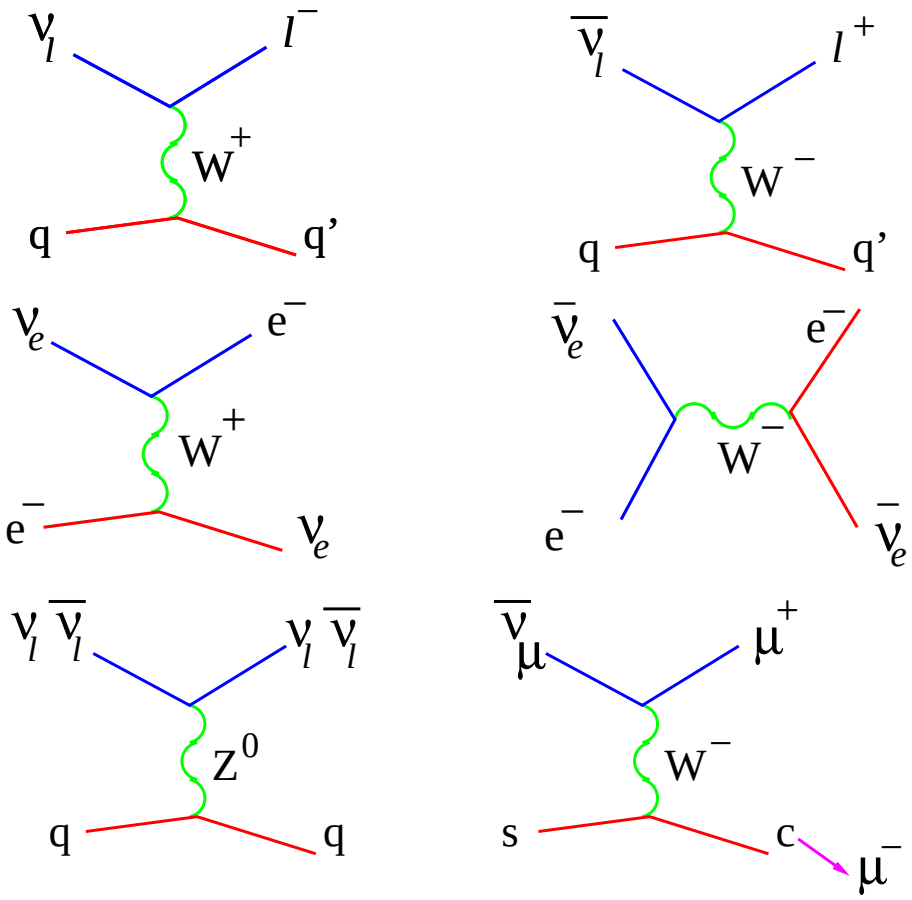

Figure 1: Feynman diagrams describing the most important neutrino interactions that will be discussed in this paper. The top four are fundamental for oscillation measurements, and the bottom two are potential sources of backgrounds in oscillation searches. *top* left(right): neutrino(antineutrino)-quark charged current interaction (deep inelastic scattering) *middle* left(right) neutrino (antineutrino)-electron elastic scatter *bottom* left: neutrino or antineutrino neutral current interaction *bottom* right: charm production in a $\bar{\nu}_\mu$ beam.

present at or above the few per mil level.

If one is trying to measure large effects this contamination is not such a big problem, but as we will describe later, the next step in neutrino oscillation physics

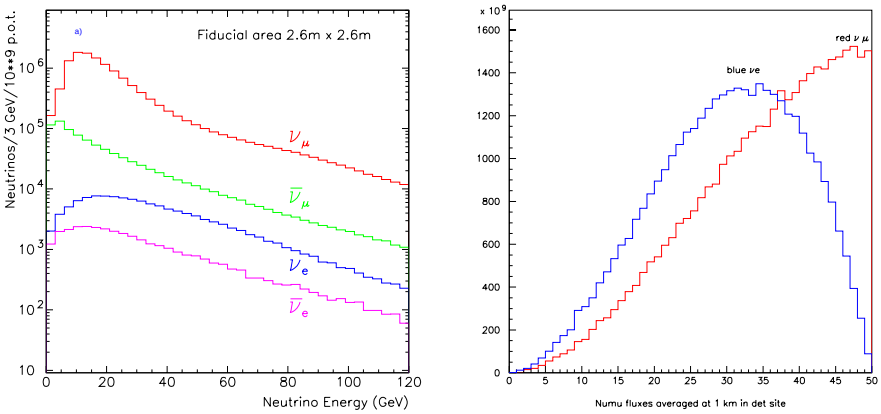

Figure 2: *left:* A conventional neutrino beam example, the SPS neutrino beam which illuminated the NOMAD and CHORUS experiments, compared with *right:* the two pure neutrino beams produced in muon decay.

will be to look for an effect which has already been determined by experiment to be less than about 5%. Precisely knowing this intrinsic background and subtracting it from a potential signal will be the only way to make the measurement in a conventional neutrino beam. Also, for most massive detectors, neutral current events, in which there is no final state muon, but an electromagnetic shower, can fake the ν_e charged current events.

Consider now the beams produced by muon decays:

$$\mu^- \to e^- \nu_\mu \bar{\nu}_e \ , \qquad \mu^+ \to e^+ \bar{\nu}_\mu \nu_e \tag{1}$$

which are shown in Fig. 2(right), for the decay of negative muons. One has *two* simultaneous beams, but now the mixture is either ν_μ and $\bar{\nu}_e$ or $\bar{\nu}_\mu$ and ν_e, and absolutely no other flavors.

Assume, for example, that negative muons are circulating in the ring. Then, a detector located downstream of the straight section will be illuminated by a beam of muon neutrinos (resulting also in negative muons in the detector) and

a beam of electron anti-neutrinos, some of which may oscillate to muon anti-neutrinos. Those, in turn, will yield positive ("wrong sign") muons (15) in the detector. There are no muon anti-neutrinos in the beam, thus, in the absence of detector misidentification (which are *much* smaller than in the conventional case), and $\nu_\mu \to \bar{\nu}_\mu$ transitions (which are even more unexpected), the observation of positively charged muons signals the existence of a $\bar{\nu}_e \to \bar{\nu}_\mu$ transition.

The final important fact to note about these measurements is that simply by measuring both $\nu_e \to \nu_\mu$, and $\bar{\nu}_e \to \bar{\nu}_\mu$, one can access all of the interesting parameters which describe the three generation unitary mixing matrix, as was first pointed out by De Rújula, Gavela and Hernández (21). So, although neutrino factories in principle allow the measurements of all possible transitions between one flavor neutrino and another, one can extract all the interesting physics precisely, by simply building a massive detector that can measure the charge and energy of muons–a well-understood well-used detector technology.

A final advantage of muon-induced neutrino beams is that they are very well understood from the theoretical point of view. In principle one would only need to know the total charge, momentum, and polarization of the stored muons, and the neutrino event rates at any distance would be precisely calculable. In practice, there is a systematic limit in the knowledge of muon induced neutrino beams from the muon beam parameters themselves such as polarization and divergence (22). This is, nonetheless, much smaller than the uncertainty of the flux of conventional beams.

Since 1997, the amount of work devoted to the study of neutrino factories has been truly amazing. After a workshop at Fermilab dedicated to muon collider studies where the concept of neutrino factory played a major role (23), three

major international workshops have been held in Lyon (24), Monterey (25) and Tsukuba (26) and hundreds of papers have been written, devoted both to machine issues and physics potential (see (27) for some recent reviews and reports concerning the latter). In this paper we offer a glimpse of this exciting new field of research. We will emphasize the most important issues rather than attempting to be fully exhaustive.

In section two we provide a short introduction to the theory of neutrino oscillations. Section three briefly describes the current evidence that neutrinos oscillate and therefore have mass. Section four is devoted to a quick review of what will be learned by neutrino oscillation experiments before a neutrino factory would start operation. In fact all three of these sections will unapologetically focus only on issues that are relevant for neutrino factory measurements, for a more complete review of both the theory and experimental evidence see reference (28). In section five we discuss the neutrino factory beams and detectors. Section six shows the resulting physics reach of these experiments. Section seven glimpses the wealth of non-oscillation neutrino physics which would also be achievable at a detector hall near the muon storage ring itself.

2 NEUTRINO OSCILLATIONS

The origin of neutrino mixing is that the eigenstates of the weak interaction do not have to be the same as the mass eigenstates. Instead, the weak eigenstates, that is, those neutrinos produced along with either muons, electrons or taus, are admixtures of states of specific mass. So, when a neutrino of a given flavor (say ν_μ) is produced with a definite energy the different mass states will propagate through space at different velocities. In time the mass eigenstates will become

out of phase with each other, so that the mixture they form will change with time. Hence, what started as a pure muon neutrino becomes a time-varying superposition of all three neutrino flavors, assuming that there are three separate mass eigenstates (28).

Consider first, for simplicity, only two neutrino families (say ν_e and ν_μ). Let us call θ the rotation angle between weak and mass eigenstates That is:

$$\begin{aligned} \nu_e &= \cos\theta\nu_1 + \sin\theta\nu_2 \\ \nu_\mu &= \cos\theta\nu_2 - \sin\theta\nu_1 \end{aligned} \tag{2}$$

The propagation of the mass eigenstates is described by wave packets of well-defined phase and group velocity. For plane waves we have:

$$|\nu_i\rangle = e^{i(kx - w_i t)} \tag{3}$$

with phase velocity

$$v_p^i = \frac{w_i}{k} = \frac{E_i}{k} \approx 1 + \frac{m_i^2}{2k^2} \tag{4}$$

where $w_i = E_i$ are the neutrino energies, $(i = 1, 2)$, k their common momentum and m_i their masses. The mass eigenstates have different phase velocities due to their mass difference.

The weak eigenstates are described by the superposition of two wave packets, corresponding to the two mass eigenstates:

$$\begin{aligned} |\nu_e(x,t)\rangle &= \cos\theta|\nu_1(x,t)\rangle + \sin\theta|\nu_2(x,t)\rangle \\ |\nu_\mu(x,t)\rangle &= \cos\theta|\nu_2(x,t)\rangle - \sin\theta|\nu_1(x,t)\rangle \end{aligned} \tag{5}$$

Due to the different phase velocity of ν_1 and ν_2 a time–dependent phase difference appears during the propagation of the mixed states ν_e and ν_μ:

$$\Delta\phi(t) = (v_p^i - v_p^j) \times k \times t = \frac{\Delta m^2}{2k} t \tag{6}$$

For small neutrino masses, the phase difference depends on the mass squared differences between the oscillating neutrinos. Therefore, for neutrinos of either vanishing or identical masses there is no time-dependent phase difference and therefore no oscillation.

From the equations above, one can derive the probabilities for a neutrino to oscillate to another flavor, or remain the same:

$$P(\nu_e \to \nu_\mu) = \sin^2 2\theta \sin^2 \frac{1.267 \Delta m^2 L}{E} \tag{7}$$

and

$$P(\nu_e \to \nu_e) = 1 - \sin^2 2\theta \sin^2 \frac{1.267 \Delta m^2 L}{E} \tag{8}$$

where, if we express Δm^2 in eV^2, then the distance L is expressed in m (km) and the energy E in MeV (GeV).

This simple picture must be modified for the case of three neutrino families. Instead of a simple one-parameter rotation matrix, we now have a 3×3 mixing matrix, U, which, if it is unitary,

$$\begin{pmatrix} \nu_e \\ \nu_\mu \\ \nu_\tau \end{pmatrix} = U \begin{pmatrix} \nu_1 \\ \nu_2 \\ \nu_3 \end{pmatrix} \tag{9}$$

can be expressed by four parameters: three mixing angles and a CP-violating phase, δ. A convenient way to parameterize it is:

$$U = \begin{pmatrix} 1 & 0 & 0 \\ 0 & c_{23} & s_{23} \\ 0 & -s_{23} & c_{23} \end{pmatrix} \begin{pmatrix} c_{13} & 0 & s_{13}e^{i\delta} \\ 0 & 1 & 0 \\ -s_{13}e^{-i\delta} & 0 & c_{13} \end{pmatrix} \begin{pmatrix} c_{12} & s_{12} & 0 \\ -s_{12} & c_{12} & 0 \\ 0 & 0 & 1 \end{pmatrix} \tag{10}$$

with $s_{12} \equiv \sin\theta_{12}$, and similarly for the other sines and cosines. Notice that this decomposition parameterizes the 3-d rotation as the product of three indepen-

dent rotations, one in the plane 23 (responsible for the atmospheric transitions), another in the plane 12 (solar transitions) and a third one that connects both. This rotation contains the angle θ_{13} which acts as a link between the atmospheric and solar realms, as well as the CP phase δ. We know from experimental data that θ_{13} is small (the CHOOZ experiment(29) has set a limit $\theta_{13} < 13^{\circ}$), and we know from solar and atmospheric experiment that there exists a strong mass hierarchy in the neutrino sector ($\Delta m^2_{atm} >> \Delta m^2_{sol}$). The consequence is that solar and atmospheric oscillations approximately decouple to two 2-by-2 mixing phenomena, as easily seen by taking the limit $\theta_{13} \to 0$, which results in the second matrix in our parameterization becoming the identity matrix. Most experiments until now have been sensitive either to the atmospheric or the solar parameters. What makes the neutrino factory unique is precisely its ability to measure, or set very stringent limits on the parameters of the second matrix in equation 10: θ_{13} and δ. Also, by having both ν_e and ν_μ beams to study, we have many more handles on the overall framework–are there really three neutrinos, and is the mixing matrix really unitary? If there is an additional sterile neutrino, then a 3×3 matrix would be an incomplete description, and therefore not unitary.

In vacuum, defining the product of the U matrix elements (often called the MNSP matrix after Maki, Nakagawa, Sakata and Pontecorvo) $W^{jk}_{\alpha\beta} \equiv [V_{\alpha j} V^*_{\beta j} V^*_{\alpha k} V_{\beta k}]$, one can generalize the two family case and write the probability of a neutrino (antineutrino) of flavor α to oscillate into a neutrino (antineutrino) of flavor β as:

$$\begin{aligned} P(\nu(\bar{\nu})_\alpha \to \nu(\bar{\nu})_\beta) &= -4 \sum_{k>j} \mathrm{Re}[\mathrm{W}^{\mathrm{jk}}_{\alpha\beta}] \sin^2\left(\frac{1.267 \Delta \mathrm{m}^2_{\mathrm{jk}} \mathrm{L}}{\mathrm{E}_\nu}\right) \\ &\pm 2 \sum_{k>j} \mathrm{Im}[\mathrm{W}^{\mathrm{jk}}_{\alpha\beta}] \sin\left(\frac{2.534 \Delta \mathrm{m}^2_{\mathrm{jk}} \mathrm{L}}{\mathrm{E}_\nu}\right) \end{aligned} \quad (11)$$

The first thing to notice is that for every transition, there is a contribution to the oscillation probability at each "frequency"– i.e. there are terms with all mass squared differences. So, if one has an experiment at some L/E near the largest Δm^2, all the transitions could in principle be accessible. Notice also that equation 11 contains a CP-even $(-4 \sum_{k>j} \mathrm{Re}[\mathrm{W}^{\mathrm{jk}}_{\alpha\beta}] \sin^2\left(\frac{1.267\Delta \mathrm{m}^2_{\mathrm{jk}}\,\mathrm{L}}{\mathrm{E}_\nu}\right))$ and a CP-odd $(\sum_{k>j} \mathrm{Im}[\mathrm{W}^{\mathrm{jk}}_{\alpha\beta}] \sin\left(\frac{2.534\Delta \mathrm{m}^2_{\mathrm{jk}}\,\mathrm{L}}{\mathrm{E}_\nu}\right))$ term. The latter term is only non-zero if there is at least a non-zero phase in the U matrix. Also, one can only observe the CP-odd term by measuring appearance probabilities–it can be shown that for the survival probabilities (i.e. when α equals β) the CP-odd term is exactly zero.

With three neutrinos we have two independent mass differences. As we will discuss in some detail in the next section, experimental data suggests at the very least the existence of a small mass difference, which we label $\Delta m^2_{12} = \Delta m^2_{sol}$ and a large mass difference, $\Delta m^2_{23} = \Delta m^2_{atm}$. Fig. 3(left) shows the mass arrangement for the "natural hierarchy" case, $\nu_1 < \nu_2 < \nu_3$, in which there are two light neutrinos separated by the small mass gap and a heavier neutrino separated from those two by the large mass gap. This picture corresponds to the naive expectation of two light neutrinos ν_1 and ν_2 (which are mostly ν_e and ν_μ) and a heavier neutrino ν_3, which is mostly ν_τ. Notice, however, that one could have the same mass differences squared if $\nu_3 < \nu_1 < \nu_2$. This is often called "inverse mass hierarchy" and its depicted in Fig. 3(right). Both are allowed by the atmospheric data, which is only a function of $|\Delta m^2_{23}|$.

In the following sections we will often refer to the possibility of measuring the "sign of Δm^2_{23}". What we mean by that is to determine whether the neutrino mass pattern is "natural" $\nu_1 < \nu_2 < \nu_3$ as in Fig. 3(left) or "inverted", $\nu_3 < \nu_1 < \nu_2$,

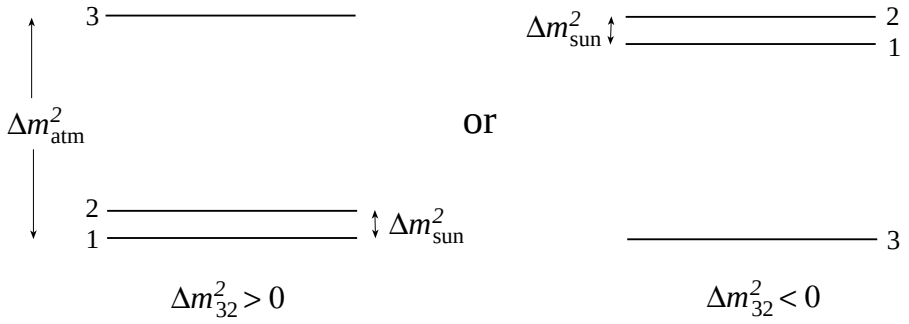

Figure 3: neutrino masses for three families. *left:* the so-called "natural hierarchy", $\nu_1 < \nu_2 < \nu_3$; *right:* the "inverse hierarchy" $\nu_3 < \nu_1 < \nu_2$.

as in Fig. 3(right).

Given the strong mass hierarchy dictated by solar and atmospheric experiments, $\Delta m^2_{atm} >> \Delta m^2_{sol}$, one can expand equation 11 if Δm^2_{sol} is sufficiently small compared with both Δm^2_{atm} and θ_{13}. In this case, equation 11 simplifies to:

$$\begin{aligned} P_{\nu_e\nu_\mu} &= \sin^2 2\,\theta_{13} \sin^2\theta_{23}\ \sin^2\frac{1.267\Delta m^2_{23}L}{E_\nu} \\ P_{\nu_e\nu_\tau} &= \sin^2 2\,\theta_{13} \cos^2\theta_{23}\ \sin^2\frac{1.267\Delta m^2_{23}L}{E_\nu} \\ P_{\nu_\mu\nu_\tau} &= \sin^2 2\,\theta_{23} \cos^2\theta_{13}\ \sin^2\frac{1.267\Delta m^2_{23}L}{E_\nu} \end{aligned} \tag{12}$$

in the system of units defined above. Notice that all the probabilities depend on only three parameters, θ_{23}, $\Delta m^2_{23} = \Delta m^2_{atm}$ and θ_{13}, and the dependence of Δm^2_{atm} is the same for all of them.

The above formulae are always a good approximation for solutions of the solar neutrino problem with very small Δm^2_{sol} (more on that in the next section). Current data, however, favors the so-called Large Mixing Angle (LMA) solution, with a most likely value for the solar mass difference of $\Delta m^2_{sol} \simeq 5 \times 10^{-5} eV^2$, which is "only" about two orders of magnitude smaller than the atmospheric mass differ-

ence. If, on the other hand, θ_{13} is sufficiently small then the approximation which leads to formulae 12 is no longer valid. Instead, a good and simple approximation for the $\nu_e \to \nu_\mu$ transition probability is obtained (30) by expanding to second order in the small parameters, $\theta_{13}, \Delta_{12}/\Delta_{13}$ and $\Delta_{12}L$, where $\Delta_{ij} \equiv \frac{2.534\Delta m^2_{ij}}{E_\nu}$,

$$\begin{aligned} P_{\nu_e\nu_\mu(\bar{\nu}_e\bar{\nu}_\mu)} &= \sin^2\theta_{23}\,\sin^2 2\theta_{13}\,\sin^2\left(\frac{\Delta_{13}\,L}{2}\right) \\ &+ \cos^2\theta_{23}\,\sin^2 2\theta_{12}\,\sin^2\left(\frac{\Delta_{12}\,L}{2}\right) \\ &+ \tilde{J}\,\cos\left(\pm\delta - \frac{\Delta_{13}\,L}{2}\right)\frac{\Delta_{12}\,L}{2}\sin\left(\frac{\Delta_{13}\,L}{2}\right), \end{aligned} \tag{13}$$

and

$$\tilde{J} \equiv cos\theta_{13}\,\sin 2\theta_{12}\sin 2\theta_{23}\sin 2\theta_{13} \tag{14}$$

is the combination of mixing angles appearing in the so-called Jarlskog determinant.

Notice that, according to equation 13, the CP-odd term is proportional to J (and therefore to the product of all the mixing angles), and also to Δm^2_{sol}. Therefore any CP asymmetry will be suppressed by the solar Δm^2 and mixing angle and will become unmeasurable if those parameters are too small, as would be the case if the solar solution does not lie in the LMA region.

Finally, the formulae above are obtained assuming propagation in vacuum. However, when neutrinos propagate through matter, as is the case for neutrinos coming out from the solar core or for neutrinos traversing the earth, there are scattering processes which can occur for which the neutrinos still propagate in the forward direction. These additional diagrams can be thought of as creating a refractive index (31), which changes the phase velocities. Since matter is full of electrons, the electron neutrinos and antineutrinos can undergo a $W^\pm$ exchange with those electrons while still propagating forward, unlike any of the other neu-

trinos (see middle diagrams in Figure 1). Because of these two diagrams, an additional phase difference appears:

$$\Delta\varphi = \sqrt{2} G_F n_e t \tag{15}$$

where n_e is the ambient electron number density.

The existence of a refraction index for electrons (and not for muons and taus) results not only in the appearance of an additional phase difference (and thus a different oscillation length) with respect to the vacuum case, but also in transitions between the vacuum states ν_1 and ν_2, which are no longer eigenstates of the Hamiltonian in matter, and have, therefore, no definite phase or group velocities. The states of definite phase velocities are the matter mass eigenstates:

$$M_\nu^2 = V_{MNSP} \begin{pmatrix} m_1^2 & & \\ & m_2^2 & \\ & & m_3^2 \end{pmatrix} V_{MNSP}^\dagger + \begin{pmatrix} \pm 2E_\nu A & & \\ & 0 & \\ & & 0 \end{pmatrix} \tag{16}$$

where $A \equiv \sqrt{2} G_F n_e$. The presence of matter modifies the transition probabilities which can be written, for example, for the $\nu_\mu \to \nu_e$ transitions as:

$$P_{\nu_e \nu_\mu (\bar{\nu}_e \bar{\nu}_\mu)} = \sin^2\theta_{23} \sin^2 2\,\theta_{13} \left(\frac{\Delta m_{23}^2}{B_\pm} \right)^2 \sin^2 \frac{1.267 B_\pm L}{E} \tag{17}$$

which has the same form as the corresponding probability in vacuum (equation 12) substituting the mass difference Δm_{atm}^2 by an "effective mass difference"

$$B_\pm \equiv \Delta m_{23}^2 \left[\left(\cos 2\,\theta_{13} \pm \frac{2E_\nu A}{\Delta m_{23}^2} \right)^2 + \sin 2\,\theta_{13}^2 \right]^{1/2}, \tag{18}$$

and the mixing angle $\sin^2 2\theta_{13}$ by an "effective mixing angle" $\sin^2 2\,\theta_{13} \left(\frac{\Delta m_{23}^2}{B_\pm} \right)$ and where B_+ is the mass difference for neutrinos, and B_- is the mass difference for antineutrinos. An early discussion of the effect this has on terrestrial long baseline experiments can be found in referece (32). Notice that if $\sin^2 2\theta_{13}$ is close to zero, and $\frac{2E_\nu A}{\Delta m_{23}^2}$ is close to one, then either B_+ or B_- will be very different from Δm_{23}^2!

For the Earth's crust, with density $\rho \sim 2.8 g/cm^3$ and roughly equal numbers of protons, neutrons and electrons, $A \sim 10^{-13} eV$. The typical neutrino energies we are considering are tens of GeV. For instance, for $E_\nu = 30$ GeV (the average $\bar{\nu}_e$ energy in the decay of $E_\mu = 50$ GeV muons) $2AE_\nu$ is $1.1 \times 10^{-4}\ eV^2$, which is close to Δ_{23}. This means that matter effects will be important at "neutrino factory" distances, as was recognized at an early stage in references (33, 34, 35). Since the "effective mass" $B_\pm$ is different for neutrinos and antineutrinos, the net effect of matter is to induce, at sufficiently large baselines, a "fake" CP-asymmetry which hides genuine CP-violation. In fact, as we will see, at sufficiently large distances, matter effects completely wash out CP-violating effects.

It turns out that very short distances are not good either. At such short distances, to first order in the ratio of the mass squared splittings, Eq. (13) can be further approximated by:

$$P_{\nu_e \nu_\mu (\bar{\nu}_e \bar{\nu}_\mu)} = \left(\frac{1.267 \delta m^2_{13} L}{E} \right)^4 \times \left[\sin^2 \theta_{23} \sin^2 2\theta_{13} + \tilde{J} r (\cos\delta \mp \sin\delta \frac{1.267 \delta m^2_{13} L}{E}) \right] \quad (19)$$

where $r = \delta m^2_{12} / \delta m^2_{13}$, and is probably no larger than 0.01. Notice that the CP-odd term in the probability (i.e. the one proportional to $\sin\delta$) is multiplied by a number much less than one even before being added to the CP-conserving $\cos\delta$ term, and both δ-dependent terms are multiplied by two small numbers: the Jarlskog determinant and r. Fortunately, there is an optimal distance (30) such that one can be both sensitive to CP and the effect is not buried by matter effects (while, on the other hand, matter effects will allow the measurement of the neutrino mass hierarchy).

In this section, we have sketched the theory of neutrino oscillations assuming

there are three generations participating in the mixing. The next section reviews in some detail the current evidence, which hints that there may be much more to oscillations than what we have outlined here.

3 EVIDENCE FOR NEUTRINO OSCILLATIONS

3.1 Evidence of Oscillations from Atmospheric Neutrinos

When cosmic rays hit the upper atmosphere, they produce hadron showers, made mainly of pions. Those pions decay to muons, $\pi^+ \rightarrow \mu^+ + \nu_\mu$, which decay in turn, $\mu^+ \rightarrow e^+ + \overline{\nu}_\mu + \nu_e$, producing the complete set of atmospheric neutrinos. Naively, one expects two muon neutrinos for each electron neutrino, thus, the expected ratio R of the flux of $\nu_\mu + \overline{\nu}_\mu$ to the flux of $\nu_e + \overline{\nu}_e$ should be about two. In fact, this ratio has been calculated in detail with an uncertainty of less than 5% over the range of energies from 0.1 GeV to 10 GeV (36, 37).

The "atmospheric neutrino problem" appeared when the observed values of R in deep underground experiments (11) turned out to be significantly smaller than two. But the fact that the atmospheric ν_μ's were disappearing was not sufficient to demonstrate that the effect was due to oscillations, since one might simply be mis-calculating the overal acceptance of the detector, the overall rate of neutrino production, etc. What turned this "problem" into a discovery is the demonstration of the right dependence on L/E (given in equations 7 and 8).

For detectors near the surface of the Earth, the neutrino flight distance, and thus the oscillation probability, is a function of the zenith angle of the neutrino direction. Vertically downward-going atmospheric neutrinos travel about 15 km while vertically upward-going atmospheric neutrinos travel about 13,000 km before interacting in the detector. Although one only measures the direction of the

final state electron or muon, these are highly correlated with the initial neutrino direction.

The historic measurement of a dependence of the atmospheric neutrino flux on the zenith angle by the Super-Kamiokande (12) collaboration is the most widely accepted evidence for neutrino oscillations. Because of their extremely massive neutrino target (50ktons of water) instrumented with phototubes to collect the Čerenkov light from electrons or muons, they were able to look at the angular dependence of both the muon-like and electron-like neutrinos. The ν_μ data exhibit a strong up-down asymmetry in zenith angle (Θ) while no significant asymmetry was observed in the ν_e data. This is illustrated in Figure 4 (from (38)) where the zenith angle distributions observed in Super-Kamiokande for sub-GeV (visible energy below 1.2 GeV) and multi-GeV (visible energy above 1.2 GeV) ν_μ and ν_e events is shown. If there is a "face that launched a thousand ships" in this field, this is it!

Early measurements of the zenith angle dependence of the atmospheric neutrino flux allowed the hypothesis of $\nu_\mu \to \nu_e$ and $\nu_\mu \to \nu_\tau$ oscillations as explanations of the data. However, the $\nu_\mu \to \nu_e$ explanation has been excluded in practice by the CHOOZ (pronounced "show") experiment, which looks for (but does not find) the disappearance of $\bar{\nu}_e$ neutrinos coming from a reactor near the village of Chooz in France (29). All recent analyses of the data (see (39) for recent work in the context of three families) agree that atmospheric neutrino oscillations can be explained in terms of $\nu_\mu \to \nu_\tau$ oscillations, with maximal or near-maximal mixing and a mass splitting of roughly $\Delta m^2_{atm} s \sim 2.2 \times 10^{-3}$ eV^2.

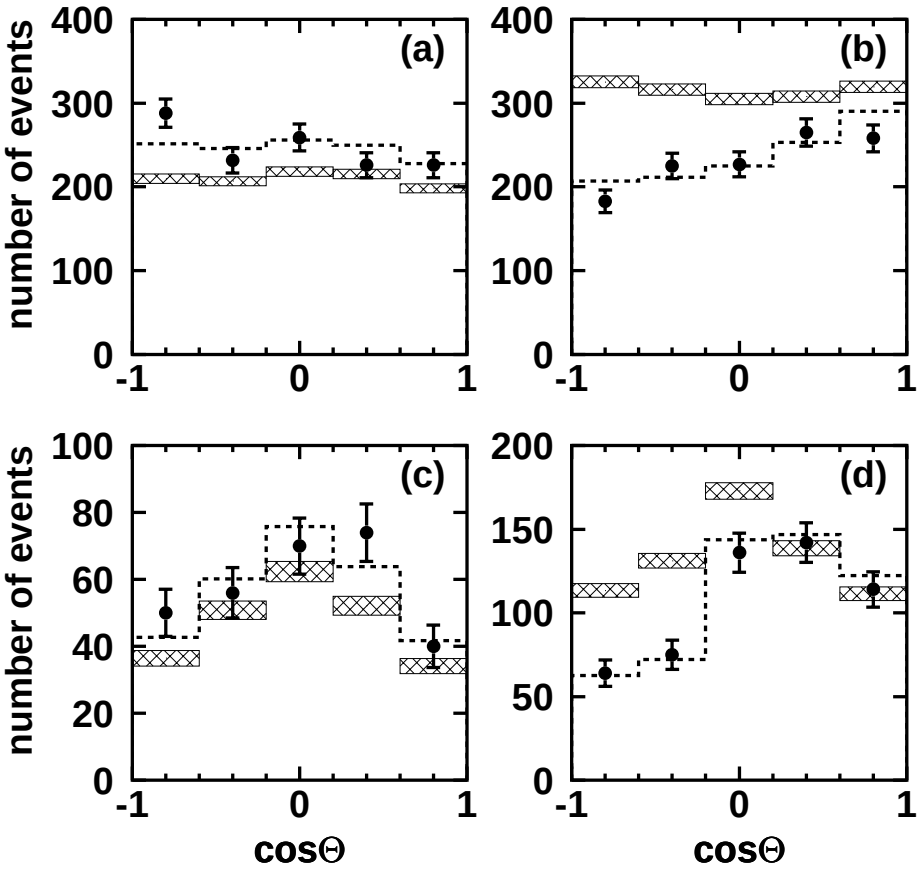

Figure 4: Zenith angle distributions observed in Super-Kamiokande for; (a)sub-GeV ν_e events, (b)sub-GeV ν_μ events, (c)multi-GeV ν_e events and (d) multi-GeV ν_μ events. $\cos\Theta$ =1 means down-going particles. The histograms with shaded error bars show the MC prediction with their statistical errors for the no neutrino oscillation case. The dotted histograms shows the Monte Carlo prediction for $\nu_\mu \leftrightarrow \nu_\tau$ oscillations with $\sin^2 2\theta$ =1 and Δm^2 $\sim 2.2\times 10^{-3}$ eV^2 (from (38)).

3.2 Evidence of Oscillations from Solar Neutrinos

The solar model (5) allows a detailed prediction of the solar neutrino rates observed by terrestrial experiments, as well as the energy spectrum and decay sources of the neutrinos. The main neutrino and energy production chain in the sun is the proton-proton–*pp*–cycle. Other secondary reactions involve the

intermediate production of Boron eight–^8B–and Beryllium seven–^7Be. See (40) for a detailed discussion. Davis's chlorine experiment (6) is sensitive mainly to ^8B and ^7Be neutrinos, and observes a rate three times smaller than predicted ($R = \Phi_{obs}/\Phi_{theo} = 0.3 \pm 0.06$). The water experiments (9), sensitive only to ^8B, observe a rate two times smaller ($R = 0.46 \pm 0.1$). The gallium experiments (7, 8), sensitive to pp,^8B and ^7Be neutrinos, observe $R = 0.6 \pm 0.1$. Finally, the SNO experiment (10, 41), whose target is deuterium (^2H_2O) and is also only sensitive to ^8B neutrinos, measures $R = 0.347 \pm 0.029$ (41). In all cases, the experimental values are significantly less than the model predictions. This deficit is the "solar neutrino problem".

The recent results from the SNO experiment have special relevance, since they have shown that the CC rate (from solar ν_e's only) in a deuterium detector is only 0.347 ± 0.029 of the standard model prediction, to be compared with the result from the Super-Kamiokande experiment, which measures the ν_e charged current rate plus–with reduced efficiency–the muon and tau neutrinos, and observes $R = 0.451 \pm 0.005$ (statistical)$^{+.016}_{-0.014}$(systematic) of the standard model prediction (9). The fact that SNO observes 3.3σ fewer neutrinos from the sun than Super-Kamiokande's total rate is evidence that some electron type neutrinos become muon and tau neutrinos after they are created in the center of the sun. This is particularly important because now the loss of neutrino rate cannot be attributed completely to some other means of disappearance, such as decay.

The explanation for the solar anomaly comes again from the hypothesis of neutrino oscillations. As for atmospheric neutrinos the literature is abundant, we refer the interested reader to (42), as well as combined analysis of atmospheric, reactor and solar data (45). Very recent work (44, 43) also includes the data from

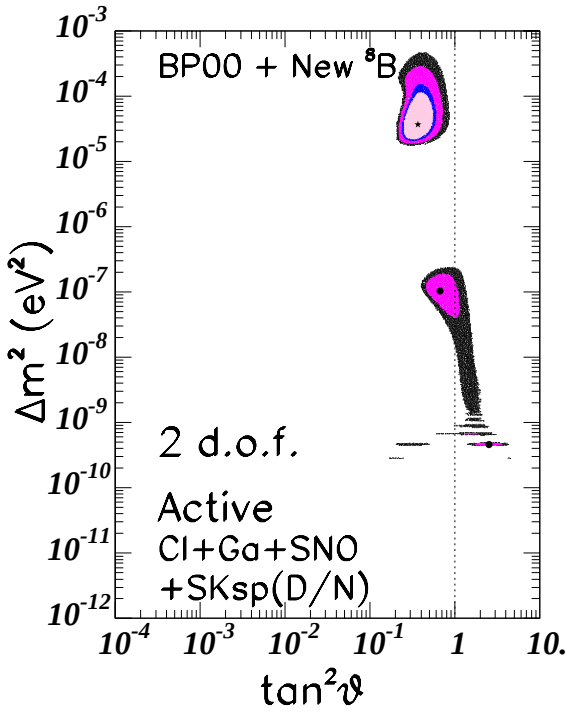

Figure 5: Results of a global fit to the solar data (from (43), assuming three active neutrinos. Notice that the preferred solution is the large mixing angle

the SNO experiment (10, 41).

Fig. 5 (from (43)) shows a global fit to solar data, taking as a theoretical reference for the solar fluxes the standard solar model (BP00) and assuming three active neutrinos. The preferred solution (called LMA, for large mixing angle) yields a relatively large splitting, $\Delta m^2_{12} \sim 5 \cdot 10^{-5}$ eV^2 and near maximal mixing angle. This, as we will later discuss, is extremely good news for the neutrino factory physics program. However, the data still allows solutions with much smaller values of Δm^2_{12}.

3.3 The LSND Result and the Hypothesis of Sterile neutrinos

In 1995, the Liquid Scintillator Neutrino Detector (LSND) experiment, operating at Los Alamos Neutron Science Center, reported an excess above background of $\bar{\nu}_e$ events in a primarily $\bar{\nu}_\mu$ beam created by the decays of stopped μ^+ particles. Since the baseline was only $30m$, this implies a squared mass difference Δm^2_{lsnd} between 0.2 and 10 eV^2. A mass difference this high implies that the at least one neutrino mass would be greater than $\sim 0.4eV$, and might be enough to account for a sizeable fraction of the mass of the universe!

If their results, along with the other two signatures, are due to oscillations one would have to assume the existence of three very different mass squared differences, $\Delta m^2_{sol} << \Delta m^2_{atm} << \Delta m^2_{lsnd}$, which cannot be explained with three neutrinos. The simplest case in which this condition is satisfied requires the existence of a fourth light neutrino, which must be *sterile* (*i.e.,* it does not couple to the weak bosons) in order not to affect the invisible Z decay width, which is precisely measured at LEP, the e^+e^- collider at CERN. Since LSND measures the appearance of electron neutrinos in a muon neutrino beam, the sterile neutrino cannot contribute very much at that mass splitting. For recent work see references (46, 47, 48).

In fact experiments have looked for sterile neutrino contributions in the disappearance signatures. One way to do this is to count neutral current events (shown at the bottom of Figure 1). Tau neutrinos would produce neutral current interactions, while sterile neutrinos would not. Based on the most recent Super-Kamiokande data (49), the muon neutrinos are disappearing to active rather than sterile neutrinos at the 99% confidence level. However, in a 4-generation mixing picture, there could be some muon neutrinos oscillating to sterile neutrinos. That

fraction must be small, as described in reference (50) and those references listed above.

There are still other explanations which can accommodate all three sets of data. However, these involve more dramatic changes in the standard model, such as CPT violation[1] (52) or extra dimensions (53) which we will not discuss any further. In the next section, we comment on how the next generation of neutrino experiments should help us to clarify the current picture.

4 THE NEXT GENERATION OF NEUTRINO OSCILLATION MEASUREMENTS

In the previous section we outlined how forty years of experimentation have led us to believe in a fifty-year-old idea, that of neutrino oscillations. We have seen that the "atmospheric anomaly" can be explained as $\nu_\mu \rightarrow \nu_\tau$ oscillations, with $\Delta m^2_{23} \sim 2 - 3 \times 10^{-3} eV^2$ and near–maximal mixing. The "solar problem", can also be explained in terms of oscillations. There are still various allowed solutions, the preferred one being LMA, with parameters $\Delta m^2_{12} \sim 5 \times 10^{-5} eV^2$ and also large mixing. The angle θ_{13}, which links the solar and atmospheric sectors, is bounded to be smaller than about 13°. All the above are at the 90% confidence level, and assuming three active neutrinos.

What remains to be learned? First and foremost, this field must resolve the remaining "anomaly", that of the LSND observation. Although somewhat marginally, all current data could be explained by introducing sterile neutrinos, if the LSND signature was in fact due to oscillations. The consequences of such

[1] Will neutrinos, invented to save energy conservation prove that sacred CPT is violated? That would be a subtle joke from Nature.

sterile neutrinos for the neutrino factory physics, in particular for the prospects of observing CP violation, are enormous (51).

The MiniBooNE experiment (54) is designed to confirm or refute unambiguously the LSND result at a completely different neutrino energy (but with a correspondingly different baseline to access the same mass squared splitting). The neutrino beam is made from protons supplied by the Fermilab Booster (hence the name). The detector consists of a 12 m sphere of scintillator-doped mineral oil instrumented with phototubes, located 50 meter from the neutrino. MiniBoooNE is scheduled to start data taking in the middle of 2002, and should obtain a clear result in less than three years. If they see a signal, the precision on the mixing matrix elements will be about 10%. In that case, an additional detector will be built, and what would then be the BooNE experiment would make a measurement of the parameters with roughly a 1% precision.

The next essential issue to clarify is whether the solar solution lies in the LMA region or elsewhere. This is crucial for the prospects measuring CP violation at a neutrino factory. As we have seen in section two, the CP-odd term is proportional to the product of all the mixing angles, and also to Δm^2_{12}. Any solution different from LMA will yield too small a mixing angle and Δm^2_{12} for a CP phase to be observable.

Fortunately, this question will also be answered in the next few years, by the KamLAND reactor neutrino experiment in the Kamioka mine (55), which is to start taking data soon. After a few years of data taking, KamLAND will be capable of either excluding the entire LMA region or, in the case of a positive signal for oscillations, not only establishing $\nu_e \leftrightarrow \nu_{\rm other}$ oscillations, but also of measuring the oscillation parameters $(\tan^2\theta_{12}, \Delta m^2_{12})$ with a precision of about

10 % (56, 57, 58).

In addition to resolving the LSND anomaly and determining if LMA describes the solar anomaly, still other future experiments are designed to improve our knowlege of the parameters governing atmospheric oscillations. These experiments have often been called "long baseline experiments", since the neutrinos travel hundreds of kilometers between source and detector.

The only one of these experiments which has taken data so far is the K2K (59) experiment, which is currently in the middle of its run. An unfortunate accident in the Super-Kamiokande detector in November 2001 [2] stopped their data taking at the time of this article, but they expect to resume running after roughly a year shutdown. The goal of K2K is to confirm the evidence of oscillations presented by Super-Kamiokande by looking for the disappearance of ν_μ's, created at the KEK laboratory in Tsukuba, Japan (hence the name: KEK to Kamiokande). The neutrino beam has a mean energy of about 1 GeV, and the beamline points to the SuperKamiokande detector, which is located 250 km from the neutrino source. Thus, the Δm^2 to which they are sensitive is:

$$\Delta m^2 \sim \frac{1GeV}{250km} \sim 4 \times 10^{-3} eV^2$$

which is near the maximum of the oscillation. The current results of K2K are consistent with those of Super-Kamiokande, although with not sufficient statistical significance to serve as confirmation.

The next long baseline experiment that will start operation is the Main Injector Neutrino Oscillation Search (MINOS) (60), which is currently under construction. Using a neutrino beam created by protons from the Fermilab Main Injector, MINOS is designed to make the first precision measurement of the parameters

[2] See http://www-sk.icrr.u-tokyo.ac.jp/doc/sk/index.html for details

governing the atmospheric neutrino anomaly. The experiment has a basline of 735 km , and the neutrino energy can be varied to produce beams of mean energies up to 14 GeV . The low energy beam, with a peak neutrino energy of 3.5 GeV will address roughly the same Δm^2 region as the K2K experiment. What distinguishes the two experiments, since L/E is comparable, is the fact that the higher statistics of the MINOS experiment will allow better precision on the oscillation parameters. The far detector, a 5 Kton sandwich with alternating slices of magnetized steel and scintillator planes, is able to clearly identify ν_μ charged current interactions and measure the total neutrino energy. The data taking is expected to start in late 2004, and after a 2 year run MINOS should be able to make a 10% measurement of the atmospheric oscillation parameters for most of the allowed range of Δ^2_{atm} (60).

The Oscillation Project with Emulsion-tRacking Apparatus (OPERA) experiment (61), housed in the Gran Sasso laboratory, in Italy, will be located at almost the exact same distance from CERN as the Soudan Mine that hosts the MINOS detector, is from Fermilab. OPERA is scheduled to start data taking in a few years using a hybrid detector, consisting of a 1.8 Kton active target made of a lead nuclear–emulsion sandwich, followed by tracking detectors. The apparatus will be illuminated by the CERN to Gran Sasso beam (CNGS). The goal of the experiment is to provide direct evidence that the atmospheric oscillation is $\nu_\mu \rightarrow \nu_\tau$ by detecting τ decays in their emulsion target. If Δm^2_{23} is $2.8 \times 10^{-3} eV^2$, then the experiment would observe about 10 τ events after 5 years of running, over a background of 0.75 events. This evidence would serve to confirm, much like the SNO experiment, that neutrinos are not disappearing, but rather are transitioning from one flavor to another. Recently the Imaging

Cosmic and Rare Underground Signal (ICARUS) collaboration (62) has made a proposal for another long base line experiment based on a 2 Kton liquid argon Time Projection Chamber, able to detect taus based on kinematical criteria, using similar techniques to those pioneered by the Neutrino Oscillation MAgnetic Detector (NOMAD) experiment at CERN (19).

Finally, we return to Japan, to mention the JHF-Kamioka neutrino project (64). This is a proposed long baseline neutrino oscillation experiment using the JHF (Japanese Hadron Facility) 50 GeV proton synchrotron, an approved facility scheduled to be complete in 2006. The machine is designed to deliver 3.3×10^{14} protons every 3.4 seconds, a stupendous intensity (0.77 MW), later to be upgraded to 4 MW (65). A high intensity almost monochromatic neutrino beam of energy around 1 GeV will be sent to Super-Kamiokande, located at 295 km from the source.

The first phase of the neutrino project could start as early as 2007. Given the enormous intensity of the beam and the large mass of Super-Kamiokande, in a 5 year run this project would provide the best knowledge of the MNSP matrix parameters before a neutrino factory. Reference (64) describes how they would achieve:

- A precision measurement of the atmospheric oscillation pattern, $\sin^2 2\theta_{23}$ with 1% precision and Δm^2_{atm} with a precision better than 10^{-4} eV^2.
- Sensitivity to a θ_{13} angle as small as $3^\circ(\sin^2 2\theta_{13} \sim 0.01)$, by searching for ν_e appearance in an almost mono-energetic ν_μ neutrino beam to reject backgrounds The expected sensitivity is an order of magnitude better than the current limit set by CHOOZ, $\sin^2 2\theta_{13} < 0.1$.

To summarize, one can reasonably expect that at the time one might start

building a neutrino factory, perhaps ten years from now, the situation will be:

- MiniBooNE will have confirmed or disproved the LSND result. For the reminder of this paper we, apologetically, assume that the LSND result will not be confirmed. It is admittedly a pessimistic assumption because the imperative for a neutrino factory becomes much stronger if it is confirmed (51).
- KamLAND will have established or excluded the LMA solution for the solar oscillation.
- long base line experiments will have measured the atmospheric oscillation parameters to a few per cent precision.
- θ_{13} will be measured if larger than about $2-3^\circ$, or an upper bound will be set.

In the remainder of this article we describe what a neutrino factory can provide in this scenario.

5 NEUTRINO FACTORY

5.1 Neutrino Beams from Muons

In the muon rest-frame, the distribution of $\overline{\nu}_\mu$ (ν_μ)and ν_e ($\overline{\nu}_e$) in the decay $\mu^\pm \to e^\pm + \nu_e(\bar{\nu}_e) + \bar{\nu}_\mu(\nu_\mu)$ is given by:

$$\frac{d^2N}{dxd\Omega} = \frac{1}{4\pi}[f_0(x) \mp \mathcal{P}_\mu f_1(x)\cos\theta]\,, \tag{20}$$

where $x = 2E_\nu/m_\mu$, and E_ν denotes the neutrino energy, m_μ the muon mass. $\mathcal{P}_\mu$ is the average muon polarization along the beam direction and θ is the angle between the neutrino momentum vector and the muon spin direction. The functions f_0 and f_1 are given in Table 1 (72).

	$f_0(x)$	$f_1(x)$
ν_μ, e	$2x^2(3-2x)$	$2x^2(1-2x)$
ν_e	$12x^2(1-x)$	$12x^2(1-x)$

Table 1: *Flux functions in the muon rest-frame as in ref. (72).*

In the laboratory frame, the neutrino fluxes per year, boosted along the muon momentum vector, are then given by:

$$\begin{aligned}
\Phi_{\nu_\mu,\bar{\nu}_\mu} = \frac{1}{L^2}\frac{d^2N_{\bar{\nu}_\mu,\nu_\mu}}{dyd\Omega} &= \frac{4n_\mu}{L^2\pi m_\mu^6}\ E_\mu^4 y^2\left(1-\beta\cos\varphi\right)\ \left\{\left[3m_\mu^2-4E_\mu^2 y\left(1-\beta\cos\varphi\right)\right]\right. \\
&\left.\mp\mathcal{P}_\mu\left[m_\mu^2-4E_\mu^2 y\left(1-\beta\cos\varphi\right)\right]\right\}, \\
\Phi_{\nu_e,\bar{\nu}_e} = \frac{1}{L^2}\frac{d^2N_{\nu_e,\bar{\nu}_e}}{dyd\Omega} &= \frac{24n_\mu}{L^2\pi m_\mu^6}\ E_\mu^4 y^2\left(1-\beta\cos\varphi\right)\ \left\{\left[m_\mu^2-2E_\mu^2 y\left(1-\beta\cos\varphi\right)\right]\right. \\
&\left.\mp\mathcal{P}_\mu\left[m_\mu^2-2E_\mu^2 y\left(1-\beta\cos\varphi\right)\right]\right\}. \qquad (21)
\end{aligned}$$

Here, $\beta=\sqrt{1-m_\mu^2/E_\mu^2}$, E_μ is the parent muon energy, $y=E_\nu/E_\mu$, n_μ is the number of useful muons per year obtained from the storage ring and L is the distance to the detector. φ is the angle between the beam axis and the direction pointing towards the detector, assumed to be located in the forward direction of the muon beam. The fluxes of ν_μ and $\overline{\nu}_e$ produced in the decay of muons of $E_\mu=10,20,50$ GeV are shown in Fig. 6. For conventional beams, the produced pion energy spectrum is steeply falling, so there is a penalty for trying to focus higher and higher energy pions which in principle also produce more focused neutrino beams. However, since neutrino factory beams are made from the muons are monochromatic, one always gets more intense beams by accelerating the muons to higher energies.

Notice, that, unlike conventional beams, the parent momentum distribution is monochromatic, so the flux at a far detector is proportional to the square of the

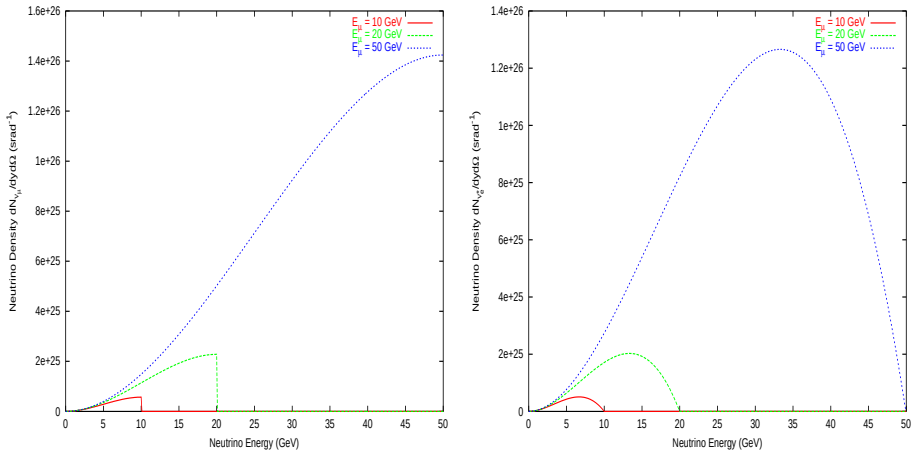

Figure 6: *left:* ν_μ and *right:* $\overline{\nu}_e$ events versus neutrino energy coming from the decay of muons of energies 10,20, and 50GeV.

average neutrino momentum.

The charged current neutrino and antineutrino interaction rates in a detector located in the forward direction of the muon beam are:

$$N_{cc}^{\nu,\bar{\nu}} = \int \Phi_{\nu_e,\nu_\mu}(E_{\nu(\bar{\nu})})\ \sigma_{\nu,\bar{\nu}}(E_{\nu(\bar{\nu})})\ dE_{\nu(\bar{\nu})}\ d\Omega \tag{22}$$

substituting the approximate expressions for the neutrino-nucleon cross sections with an isoscalar target,

$$\sigma_{\nu N} \approx \sigma_0^{\nu} \times \frac{E_\nu}{\mathrm{GeV}} \times \mathrm{m}^2\ , \qquad \sigma_{\bar{\nu} N} \approx \sigma_0^{\overline{\nu}} \times \frac{E_\nu}{\mathrm{GeV}} \times \mathrm{m}^2. \tag{23}$$

we obtain:

$$N_{cc}^{\nu,\bar{\nu}} = \sigma_0^{\nu,\overline{\nu}} \int \Phi_{\nu,\bar{\nu}}(E_{\nu,\bar{\nu}})\ E_{\nu,\bar{\nu}}\ dE_{\nu,\bar{\nu}}\ d\Omega. \tag{24}$$

where $\sigma_0^{\nu,\overline{\nu}} = 0.67(0.34) \times 10^{-42}$. It follows that the number of charged current (CC) events at a neutrino factory scales as the cube of the neutrino (and thus with the muon storage ring) energy: $N_{CC} \propto E_\mu^3$.

But what is relevant for oscillation physics is the number of *oscillated events* above background. For an appearance experiment, the oscillation probability

is a function of the leading mass squared difference (taking for simplicity the 2 generation formula):

$$P(\nu_e \to \nu_\mu) = \sin^2 2\theta_{atm} \sin^2 \frac{1.267 \Delta m^2_{atm} L}{E}.$$

The number of ν_μ's in our detector produced by ν_e oscillation will be:

$$N^{\nu_\mu}_{cc} = \sigma^{\nu\overline{\nu}}_0 \int \Phi_{\nu_e}(E)\ E\ P(\nu_e \to \nu_\mu) dE\ d\Omega =$$
$$\sigma^{\nu\overline{\nu}}_0\ \sin^2 2\theta \int \Phi_{\nu_e}(E)\ E\ \sin^2(\tfrac{1.267 \Delta \mathrm{m}^2_{\mathrm{atm}} \mathrm{L}}{\mathrm{E}}) dE\ d\Omega.$$

Assume now that the distance between detector and source is such that

$$\sin^2(\frac{1.267 \Delta \mathrm{m}^2_{\mathrm{atm}} \mathrm{L}}{\mathrm{E}}) << 1 \Rightarrow \Delta \mathrm{m}^2_{\mathrm{atm}} << \frac{\mathrm{E}}{\mathrm{L}},$$

Then, $\sin x \sim x$ and:

$$N^{\nu_\mu}_{cc} \sigma^{\nu\overline{\nu}}_0\ \sin^2 2\theta\ (1.267 \Delta \mathrm{m}^2_{\mathrm{atm}} L^2)^2 \int \frac{\Phi_{\nu_e}(E)}{E} dE\ d\Omega.$$

Since $\Phi_{\nu_e,\nu_\mu} \propto E^2$, the number of oscillated events grows linearly with the neutrino and muon storage ring energies. Conversely, the fractional number of background events (background events divided by total events in the absence of oscillations) is flat as a function of distance. As will be shown in a later section, the background rejection is very much a function of the detector, but for most detectors the backgrounds are easier to identify at higher neutrino energy.

A simple formula to compute rates of charged current events is readily obtained from the previous formulae (69):

$$N_\nu \sim f(\nu) \frac{n_\mu[10^{21}] E^3[GeV^3] M_D[kt]}{L^2 (10^3 km)^2} \tag{25}$$

where M_D is the detector mass (in kilotons). For $\nu = \nu_\mu, \nu_e, \overline{\nu}_\mu, \overline{\nu}_e$, $f(\nu) = 8, 7, 4, 3.5$ respectively.

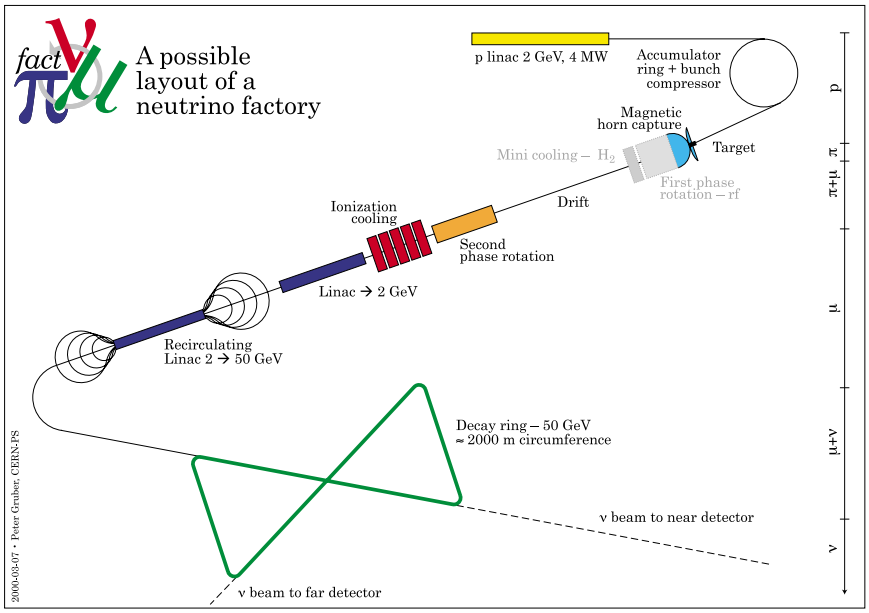

Figure 7: Layout of a neutrino factory. The figure shows the CERN design, but most elements are common to the various existing designs. See text for discussion.

5.2 Sketch of a Neutrino Factory Facility

As was understood even in the early days of neutrino storage ring designs, getting 10^{21} or a "milimole" of muons to circulate in a storage ring is a challenging task. On the other hand, we as a field are now used to manipulating much higher power proton beams than ever before, and feasability studies conducted in the United States (67, 68), Europe (66), and Japan (69) have shown at least on paper how this challenge could be met. A vigorous R& D program is underway, but must continue to be pursued to bring these designs from paper to reality.

To make a neutrino factory one must first produce an intense proton beam and then let it hit a target where it will produce pions. The proton beam, focused on the target, has a mean beam power of several MW and is produced by a high intensity proton source. There are several scenarios for the source, ranging from

a 2 GeV linac shown in Figure 7 (66),to a 16 GeV synchrotron (67)(68), all the way to a 50 GeV synchrotron (69). The target has to withstand an enormous amount of power, so one idea is to use a liquid mercury jet which would disperse well after the proton beam has left. The produced pions must then be collected in either a high field solenoid or a magnetic horn.

By the time most of the pions have decayed, the daughter muons are spread over several meters. Their distribution contains a very large momentum spread similar to that of the parent pions, correlated with position: fast muons in front, slow muons in back. In the US and CERN designs, a system of RF cavities manipulates this distribution in longitudinal phase space to reduce the energy spread by accelerating the late particles and decelerating the early particles, called *phase rotation*. After phase rotation the muons are captured into RF buckets to produce a train of muon bunches. The transverse beam phase space is then reduced using *ionization cooling*, where particles traverse a low-Z medium, such as Helium and lose energy, followed by RF acceleration, when the longitudinal momentum is restored. This cooling is the most challenging accelerator aspect of the machine, and is the innovation that makes intense cold muon sources feasible.

Next, the muons, cooled or not, must be accelerated. The Japanese design uses something called a "Fixed Field Alternating Gradient" which uses circular rings of magnets with very large apertures. By making the magnetic field higher at higher radii, the particles can be made to accelerate as they make successive turns around the ring and still stay in the machine. The US and CERN designs use a system of one or more recircululating linacs, where with each successive turn the muons are accelerated to a higher energy.

Finally, the high energy muons are injected into a storage ring. The simplest

"ring" would have two several hundred meter straight sections connected by two arcs. The drawback of this simple design is that only one straight section can point to a far detector and thus only one baseline is possible. The "bow-tie" design shown at the bottom of fig. 7, has straight sections pointing toward two different directions, allowing two experiments at two different locations. As we will see, having measurements at two baselines is important if one wants the most precise measurement of CP violation. If the neutrino beams were at shallow angles to go short distances, one could envision having two detectors both near the surface of the earth, one closer to the proton source than the other, but for the distances we are considering here one experiment would be prohibitively deep underground. It should be noted that at the stage when the muons enter the storage ring they are a well-behaved packet of particles, and the beam optics involved at this stage are not challenging compared to everything else up to this point.

5.3 Detectors

Although in principle one would like to measure all of the transitions in neutrino osclilations, remember that one can have access to the largest unknowns by simply detecting the transitions of electron neutrinos and antineutrinos to muon neutrinos and antineutrinos. The only requirement therefore is that a detector needs to be very massive, and it must be capable of identifying at the very least, an outgoing muon and its charge. We briefly discuss two technologies, one of them simple and well understood (magnetized iron calorimeter), the other far more ambitious, but which would allow more than simply transitions with muon neutrinos in the final state (liquid argon TPC). It must be noted, however, that the largest liquid argon TPC built to date is about a factor ten less massive than

the largest magnetized iron calorimeter, and considerably more expensive per kiloton than magnetized iron.

We do not discuss water detectors, which, while extremely well suited for neutrino physics in the range of about 1 GeV , are much less effective for neutrino energies in the range of the tens of GeV . The interested reader can see reference (74) for preliminary studies for how this detector might perform. This might be interesting, since in contrast to the liquid argon TPC case, the largest water cerenkov detector built to date is a factor of ten *more* massive than the largest magnetized iron calorimeter. Unfortunately, however, the cost of adding magnetized detectors to measure the muon charge is likely to be as expensive as building a massive magnetized iron calorimeter in the first place.

5.3.1 **Magnetized Iron Detectors**

The simplest and cheapest technology available to measure ν_μ and $\bar{\nu}_\mu$ charged current interactions is magnetized iron calorimetry. This is simply planes of steel magnetized by some coil, interspersed with an active medium, usually scintillator. While this kind of detector has been used for several generations of neutrino experiments in the past, it is also going to be used in the current generation, namely by MINOS (60). A detector for the neutrino factory could be identical to MINOS. For most of the physics performance calculations described in this document, the MINOS detector performance was assumed, but with a mass of 50 Kton .

Neutrino interactions have a clear signature. A charged current ν_μ event is characterized by a muon, easily seen as a penetrating track of typically several meters length, and a shower resulting from the interactions of the final-state

hadrons. The total energy of the neutrino is simply the sum of the muon and hadronic energy. As will be discussed in a later section, some measurement of the outgoing angles of the hadronic shower and the muon will also be useful for background rejection. The hadronic energy resolution for the MINOS detector is roughly $\sigma_E/E = 50\%/\sqrt{E(GeV)}$ and the muon momentum resolution is typically $\sigma_p/p = 11\%$ (60).

A neutral current event contains no penetrating track and the length of the event is the length of the hadron shower in iron, typically less than one meter. CC ν_e events cannot be easily recognized since, with a detector of this coarse granularity, it is difficult to disentangle the prompt electron from the hadronic shower on an event-by-event basis.

5.3.2 **Liquid Argon TPC**

A magnetized iron calorimeter can measure wrong sign muons and thus has access to all the parameters of the MNSP matrix. However, if a large facility like the neutrino factory is built, one would like to have additional detectors able to see the other signatures readily available from muon beams: "wrong sign taus" and "wrong sign electrons".

A massive imaging device such as a liquid argon time projection chamber (TPC), à la ICARUS (76), could be sensitive,*a priori* to the above signatures. A liquid argon TPC produces essentially bubble chamber quality reconstructed events and can easily separate muons (penetrating, minimum-ionizing tracks) from pions (shorter tracks which end in a broad shower) and electrons (even shorter tracks, followed by a narrow shower). The 600 ton ICARUS module (76) is instrumented with 3 mm pitch wires. These allow tracking, dE/dx measure-

ments, and electromagnetic and hadronic calorimetry. Electrons and photons can be identified event by event, and their energies are measured with a resolution given by $\sigma_E/E = 3\%/\sqrt{E(GeV)} \oplus 1\%$. The hadron energy resolution is given by $\sigma_E/E = 20\%/\sqrt{E(GeV)} \oplus 5\%$. The symbol $\oplus$ means "added in quadrature".

However, one still needs to measure the charge of the outgoing lepton in the charged current events. Muons are penetrating; thus, they can be measured by interspersing magnetized iron segments between few-meter long segments of liquid argon. This results in a hybrid detector (liquid argon + magnetized iron) which would be able to provide several consistency checks to the oscillation measurement (77), and searches for "wrong sign taus" by using the $\tau \to \mu$ decay. Also, if one were to change the muon beam polarization and hence the ν_e content in the beam, one might be able to do clean $\nu_\mu \to \nu_e$ measurements (see (78)). However, the biggest drawback is the cost of such a device.

An alternative would be to have a magnetic field in the detector volume itself, for example by embedding the TPC in a large solenoid (82). Then one would have a continuous magnetized *granular* calorimeter, which could in principle separate both $\mu^+/\mu^- and\, e^+/e^-$. Indeed, this would be the ideal device for neutrino factory physics.

The problem, alas, is how to create a magnetic field in such an enormous volume (recall that one needs tens of Kton to be sensitive to CP violation, and that the density of liquid argon is a factor of three less than the density of the MINOS detector). The largest liquid argon device built so far has a mass of 0.6 Kton , while the largest iron calorimeter (being built), MINOS, has an order of magnitude more mass, 5 Kton. Furthermore, the former has no magnetic field, and the latter is made of magnetized iron. Building a 50 Kton iron detector is by

Baseline (km)	$\overline{\nu}_\mu$ CC	ν_e CC	$\overline{\nu}_\mu + \nu_e$ NC	ν_μ(signal)
732	3.5×10^7	5.9×10^7	3.1×10^7	1.1×10^5
3500	1.5×10^6	2.6×10^6	1.3×10^6	1.0×10^5
7332	3.5×10^5	5.9×10^5	3.0×10^5	3.8×10^4

Table 2: *Data samples expected in a 40* Kton *fiducial mass detector for* 10^{21} *useful* μ^+ *decays.* $\nu_e \to \nu_\mu$ *oscillations with* $\theta_{13} = 13^\circ$ *and the LMA solution.*

no means easy, but one would dare to say, a straight-forward extrapolation of a well-known modular technology. Building a 10-50 Kton magnetized liquid argon TPC represents, in our opinion, a large technological break-through. However, the neutrino factory will not be operating tomorrow. Perhaps in the next decade this break-through can be made.

5.4 Suppression of Detector-Related Backgrounds

As we have stated often, there are no direct beam backgrounds for the wrong sign muon search in a neutrino factory. However, we must still demonstrate that detector-induced backgrounds can be controlled to a satisfactory level.

Let us consider the ($\overline{\nu}_\mu$, ν_e) neutrino beams originating from a μ^+ beam of $E_\mu = 50$ GeV (the dependence of the detector-related backgrounds with the energy of the muon beam was discussed in (75), where it was shown that optimal performance is obtained at the highest possible energy). The bulk of the events in the detector are $\overline{\nu}_\mu$ charged currents, signaled by the presence of a positive primary muon in the event, $\overline{\nu}_\mu$ and ν_e neutral current events, which are events with no primary leptons, and ν_e charged current events, for which the analysis in (75) assumed that primary electrons were not identified. On top of those events,

one searches for wrong sign μ^- arising from the ν_μ produced via the oscillation $\nu_e \to \nu_\mu$.

To gain an idea of the needed background suppression level, Table 2 shows the number of interactions corresponding to a total of 10^{21} μ^+ decays in the straight section pointing to the 40 Kton far detector, for three reference baselines: "near" (732 km), "intermediate" (3500 km) and "far" (7332 km). 732 km corresponds roughly to the Fermilab-Soudan or CERN-Gran Sasso distance, and 7332 km corresponds roughly to the Fermilab-Gran Sasso distance or the CERN-Soudan distance. To compute the number of oscillated events one needs to fix a set of oscillation parameters. In the table, the chosen parameters were: $\Delta m^2_{23} = 4 \times 10^{-3}\mathrm{eV}^2$, $\Delta m^2_{12} = 10^{-4}$ eV^2, $\theta_{13} = 13^\circ$, $\theta_{12} = 22.5^\circ$ and $\theta_{23} = 45^\circ$. This set is chosen for illustration and has no particular meaning except that of illustrating the very high interaction rates expected in a neutrino factory at full performance. In fact, it represents an extreme case of good luck, with the solar solution in the upper allowed limit, a high value for Δm^2_{atm}, and θ_{13} at the allowed limit from CHOOZ.

The potential backgrounds to the wrong sign μ^- events signaling the presence of oscillations stem most importantly from the diagrams shown at the bottom of Figure 1. They are:

1. $\overline{\nu}_\mu$ CC events in which the positive muon is not detected, and a secondary negative muon arising from the decays of π^-, K^- and D^- hadrons fake the signal. The most dangerous events are those with $D^- \to \mu^-$, which yield an energetic muon with a spectrum similar to the signal.

2. ν_e CC events, for which it is assumed that the primary electron is never detected. Charm production is not relevant for this type of event, since the

charmed hadrons in the hadronic jet are predominantly positive. Instead, fake μ^-'s arise from the decay of negative pions and kaons in hadronic jets.

3. $\overline{\nu}_\mu$ and ν_e NC events. Fake μ^-'s arise in this case also predominantly from the decay of negative pions and kaons, since charm production is suppressed with respect to the case of CC.

4. "right sign" CC events in which the muon charge is wrongly measured to be of opposite sign.

At first sight these backgrounds seem impressive. If one had a very fine-grained detector, such as a liquid argon TPC, one could simply look at the primary vertex, and require that the outgoing muon emerge from that vertex rather than from the hadron shower vertex, which is likely to begin significantly downstream of the primary vertex. However, even with a coarse-grained detector such as steel-scintillator sandwich like MINOS, simple kinematical cuts can suppress these backgrounds efficiently. One again exploits the fact that for signal events the μ^- candidate is much more energetic and isolated from the hadronic shower than for background events. In (75, 30) a simple analysis is performed, based on two variables. These are: the momentum of the muon, P_μ, and a variable measuring the isolation of the muon, $Q_t = P_\mu \sin\theta$, where θ is the angle between the hadronic shower direction and the muon direction.

To illustrate the rejection power of these criteria in a steel scintillator detector, fig. 8 shows the efficiency for signal detection and the fractional backgrounds as a function of P_μ and Q_t for $\overline{\nu}_\mu$ charged and neutral currents. Also shown is the signal-to-noise ratio, S/N, defined as the ratio of the signal selection efficiency S, to N, the error in the subtraction of the number of background events that pass the cuts, ($N = \sqrt{N_b}$). Notice that charm production is the dominant background

from $\overline{\nu}_\mu$ charged current interactions, while π decay is the dominant source from neutral current interactions. The sample has been pre-selected in order to guarantee an essentially null muon-charge misidentification, by imposing that the muon track has to be longer than seven meters. In practice, this pre-selection is equivalent to a momentum cut of several GeV , but the low momentum bin considered in the analysis (from 0 to 5 GeV) is not fully depleted by this selection criterion. The efficiency and S/N are normalized by the small number of signal events passing the seven meter muon length cut. If the normalization were to the total number of events instead, one would see a very dramatic drop in the signal efficiency as the muon momentum cut moved from 0 to a few GeV, because at very low muon momentum muons cannot be separated from hadrons, which can be of either charge.

Inspection of Fig. 8 shows that cutting, for example at $P_\mu > 7.5$ GeV, $Q_t > 1.0$ GeV, yields S/N near maximal. This, together with the pre-selection of very long tracks, also results in negligible charge confusion. The residual backgrounds after the above cuts are made are quite sizable at $L = 732$km, small at $L = 3500$km and negligible at $L = 7332$km.

One might ask how these backgrounds would differ if the target material were different from steel (for example in a water Čerenkov detector). The less dense the neutrino target, the more likely the pions and kaons produced in the hadronic shower will decay to muons before interacting in the target. Reference (83) shows that with a 7.5 GeV muon momentum cut alone at a 50 GeV neutrino factory the backgrounds in water would be about 25% higher than in steel scintillator. Backgrounds from charm meson decays, however, would be idependent of target material in a coarse detector, since the charm meson decays well before it would

$\overline{\nu}_\mu$Charged Currents

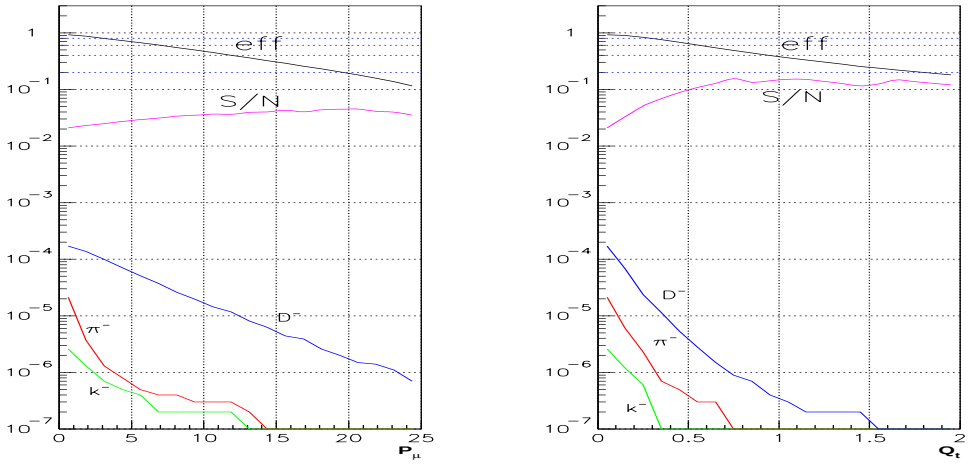

$\overline{\nu}_\mu$Neutral Currents

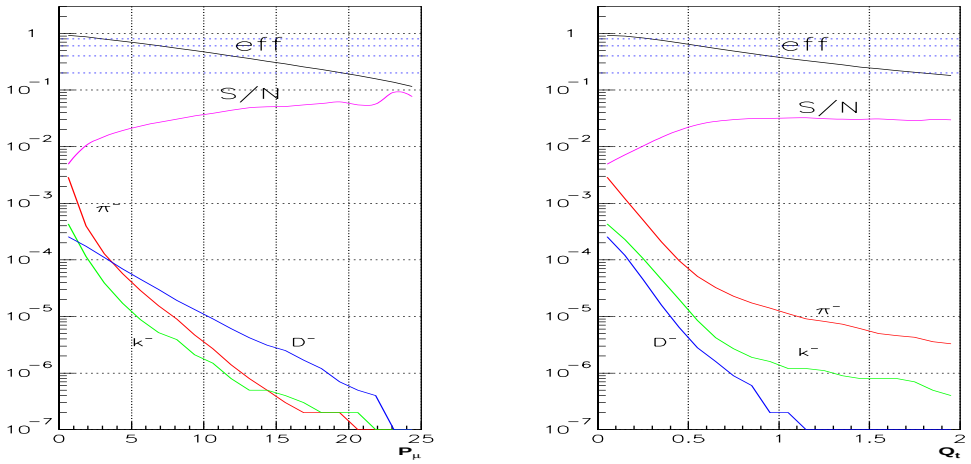

Figure 8: *Signal Efficiency (S) and fractional backgrounds as a function of an analysis cut on the momentum of the muon (p_μ) or the momentum of the muon transverse to the hadronic shower(Q_t). The backgrounds from D, π and K decays are shown separately, and the line marked S/N refers to the signal efficiency divided by the fractional error on the background events. Backgrounds from charged and neutral current processes are shown separately.*

Baseline (km)	$\overline{\nu}_\mu$ CC	ν_e CC	$\overline{\nu}_\mu + \nu_e$NC	ν_μ(signal)
732	3.5	30	31	3.3×10^4
3500	0.1	1.2	1.2	3×10^4
7332	< 0.1	< 0.2	< 0.2	1.3×10^4

Table 3: *Events surviving the cuts in a 40* Kton *detector for* 10^{21} *useful* μ^+ *decays. Oscillation parameters are defined in the text.*

initiate a hadronic shower.

At lower neutrino energies, the situation becomes more complicated. It was shown in (75) that backgrounds and charge misidentification grow exponentially for neutrino factories storing muons of less than about 20 GeV , since one cannot impose the dramatic cuts in track length, momentum and Q_t needed to reject backgrounds efficiently. Even for a 20 GeV muon storage ring the backgrounds in a water detector are much higher than in a steel detector (83).

The same exercise can be repeated when a μ^- beam is considered. The resulting neutrino beams are then ν_μ and $\overline{\nu}_e$ and the signal events are $\overline{\nu}_\mu$. Similar results are obtained, and we refer the reader to (75, 30) for further discussion.

In summary, a large magnetized iron calorimeter allows the detection, with high efficiency ($\sim 20 - 30\%$) of the gold-plated wrong-sign muon signal. The different backgrounds to this signal can be efficiently controlled using simple cuts, which exploit the very different kinematics between signal and background events. The backgrounds are better controlled at high neutrino (thus stored muon) energy, which in practice limits the minimum practical energy of a muon storage ring to about 20 GeV .

5.5 Optimizing Neutrino Factory Parameters

Now that we have described the beamline, the detectors, and the backgrounds, we can consider what is required for a discovery machine, namely:

- What physics measurements are accessible as a function of the number of useful decays (defined as muons which decay in the straight sections pointing toward the detector)?
- What is the optimal energy for the stored muons?
- Is one baseline enough or is there a case to be made for two?
- What are the optimal distances between source and detector?
- Is there a case for polarization?

Some of the answers we have already pointed out. In order to control the different backgrounds and ensure proper charge identification, the energy of the stored muons cannot be too small. In practice, this sets the minimum muon storage ring energy to about 20 GeV (75, 73). The maximum practical energy of the neutrino factory, on the other hand, is dictated by the complexity of the re-circulating linac complex, probably to a value of about 50GeV.

Fig. 9 shows the discovery potential of the neutrino factory as a function of the number of muon decays per year and of the energy of the stored muons, assuming $\sin^2 2\theta_{13} = 0.04$ (recall that the current limit at 90% confidence level is $\sin^2 2\theta_{13} = 0.1$) (88). Notice that, to observe $\nu_e \to \nu_\mu$ oscillations and determine the neutrino mass pattern, one needs about 2×10^{18} for the minimum practical energy of 20GeV and about 7×10^{17} for the maximum practical muon energy of 50GeV, in both cases for a 50 Kton detector. Observation of $\nu_e \to \nu_\tau$ oscillations with a few Kton detector would require at least 10^{20} decays. CP violation requires

about 10^{21} decays.

How do the above statements depend on the value of θ_{13}? The answer is very simple. As shown in equation 12, the subleading transition probabilities scale with $\sin^2 2\theta_{13}$. Therefore, if this mixing angle turns out to be a factor, say, ten smaller, then in the absence of backgrounds the number of muons decays needed for the observation of the subleading transitions must simply be increased by a factor of ten. However, this statement is not true for the observation of CP violation, which is almost independent of the actual value of θ_{13}, provided that it is above 1° (or $\sin^2 2\theta_{13} > 0.001$). This is because in this regime the CP-violating difference in oscillation probability is proportional to $\sin 2\theta_{13}$, while the error on the difference is (in the absence of backgrounds) proportional to the square root of $\sin^2 2\theta_{13}$. So in the ratio of the CP-violating difference and the error on that difference, $\sin 2\theta_{13}$ cancels.

Recall from the previous section that JHF expects to be sensitive to values of $\sin^2 2\theta_{13}$ as small as 0.01. If they do not observe a signal, then, a next-generation experiment neutrino factory should explore at least another order of magnitude in $\sin^2 2\theta_{13}$. The minimum number of muon decays needed, assuming negative results from JHF, will be $\sim 10^{20}$. On the other hand, CP violation may still be observed with $\sim 10^{21}$ muon decays.

What about baselines? In the next section we will make the argument that two different distances are preferable, one at the "intermediate" distance from the source of about 3000 km and a second one either "near" (O(1000km)) or "far" (O(7000km)).

Do we need the muons to be polarized? Fig. 10 shows the event energy distributions for 100% polarization both parallel and antiparallel to the beam

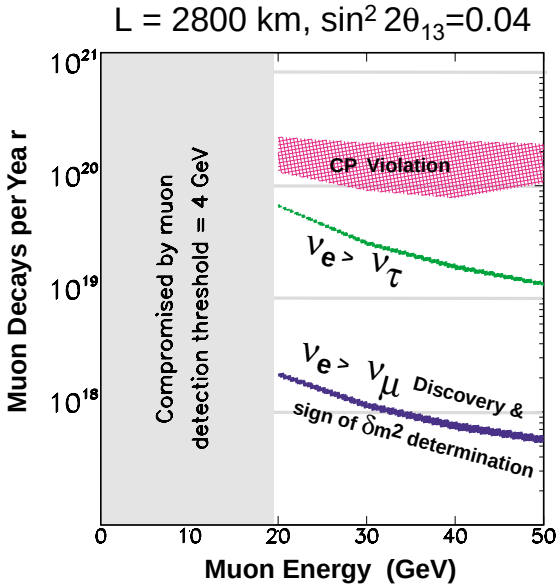

Figure 9: The required number of muon decays needed in a neutrino factory to a) observe $\nu_e \to \nu_\mu$ oscillations in a 50 Kton ($\nu_e \to \nu_\tau$ oscillations in a 5 Kton detector), b) determine the sign of Δm^2_{23}, and c)observe or set stringent limits on CP violation in the lepton sector. Results are from Ref. (88).

direction, for both μ^+ and μ^- circulating in the ring. These plots show that by varying the polarization, one can sizeably change the electron neutrino flux at the far detector, while changing only slightly the muon neutrino flux (78).

One possible application would be the observation of $\nu_\mu \to \nu_e$ oscillations, when the signal consists of appearance of CC ν_e events,with a high energy electron. Reference (79) discusses a simple event-counting analysis to search for T violation by comparing $\nu_e \to \nu_\mu$ with $\nu_\mu \to \nu_e$. In this case, the detector would not have to distinguish the sign of the electrons, one would just have to run at different muon polarizations in the storage ring. However, one must also consider possible backgrounds to a ν_e search here. One possible handle on the background is that the spectrum of the ν_e signal events would be very different from that of the background, which would originate primarily from neutral current events.

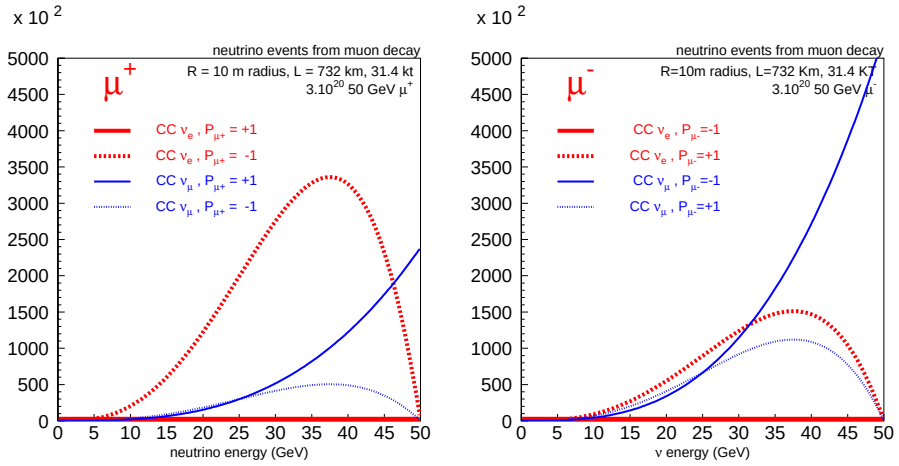

Figure 10: Event numbers for a 31.4kton, 10m radius detector situated 732 km away from the neutrino source, for 50GeV $\mu^+ \to e^+\bar{\nu}_\mu\nu_e$ (left) and $\mu^- \to e^-\nu_\mu\bar{\nu}_e$ (right) decays. Solid lines show the spectra for "natural helicity", P =+1 for $\mu^+$and dashed ones for the opposite.The charged current (CC) ν_e for μ^+ with P =+1 and CC ν_e for μ^- with P = -1 are not visible, because the flux is almost exactly zero. Results are from Ref. (78).

However, achieving and maintaining a significant level of polarization in the circulating muon beam is not easy, and it certainly contributes little to the wrong sign muon search. Furthermore, incomplete knowledge of the polarization would result in a flux uncertainty of ν_e's at the far detector (22).

To summarize, the physics program at a neutrino factory requires at the bare minimum:

- No less than 10^{18} and about 10^{20} (if JHF has not seen a signal) useful muon decays to observe $\nu_\mu \to \nu_e$ oscillations and establish the neutrino mass pattern
- A minimum energy of 20 GeV to clearly identify wrong sign muons
- a very massive ($\sim$ 50Kton) magnetized detector to study $\nu_e \to \nu_\mu$ and

$\bar{\nu}_e \to \bar{\nu}_\mu$

In the following section we describe what is necessary to go from a discovery machine to a facility which can map out precisely the leptonic mixing matrix itself.

6 PHYSICS REACH

In this section we consider a full-performance neutrino factory, defined as one providing 2×10^{20} useful muon decays in the ring per year, with muon energies from 20 to 50 GeV. A "full statistics" run will correspond to 10 data-taking years (a total of 5 years or 10^{21} μ^+ and 5 years or 10^{21} μ^- useful decays) and a MINOS-like detector of 50 Kton , unless noted otherwise. Such a facility has four major goals:

- Precision measurement of the atmospheric oscillation parameters.
- Measurement or stringent limits on the θ_{13} mixing angle.
- Establishing the neutrino mass hierarchy, by measuring matter effects.
- Observation of or stringent limits on CP-violation

Although this list of goals may seem straightforward at first glance, in fact the physics reach in each goal depends at least somewhat on what has been achieved in the previous goal. For example, although measuring the parameters of atmospheric oscillation does not depend much on other elements in the MNSP matrix, the reach in θ_{13} depends roughly on what the atmospheric mass splitting is, the determination of matter effects depends on how large θ_{13} is, and finally, the observation of or limits on CP violation depends on everything: all the mass splittings, all the mixing angles, and on the neutrino mass hierarchy and the precise size of

the matter effect itself.

For the reminder of this section, we will assume, unless explicitly stated otherwise, that Nature has been kind enough to choose the LMA solution for the solar parameters. Otherwise, CP-violation would be out of reach. Besides its capability to reduce the errors on θ_{23} and $|\Delta m^2_{23}|$ to $\sim 1\%$, the neutrino factory would still be a unique machine to constrain/measure θ_{13} (21) and the sign of Δm^2_{23} (89, 90, 88, 33). We will also assume that nature nas not been so kind as to permit a higher mass splitting, such as the one currently suggested by the LSND case. As was stated earlier, if in fact there are three mass scales and at least one fourth sterile neutrino, the motivation for a neutrino factory increases manyfold: the possibilities for measuring CP violation at short baselines become enormous (for example in $\nu_e \to \nu_\tau$ versus $\bar{\nu}_e \to \bar{\nu}_\tau$) (51), while the requirements on the number of muon decays per year are significantly reduced.

6.1 Measurement of the Atmospheric Parameters

The atmospheric parameters $(\Delta m^2_{23}, \sin^2 2\theta_{23})$ are expected to be measured to about 10 % precision by MINOS and hopefully to a few per cent by JHF. A neutrino factory can further improve in precision, to the 1% level or better.

The best determination of the atmospheric parameters is done by simply counting "right sign" muons and comparing with the expectations. Reference (22) gives the expected flux uncertainties due to imperfect knowlege of the details of the muon beam, for example beam divergence or polarization. With the presence of a near detector the detector effects can be very well-understood. Thus one knows with very good precision the expected event rates in the absence of oscillations. This, together with the very high statistics, results in a high precision

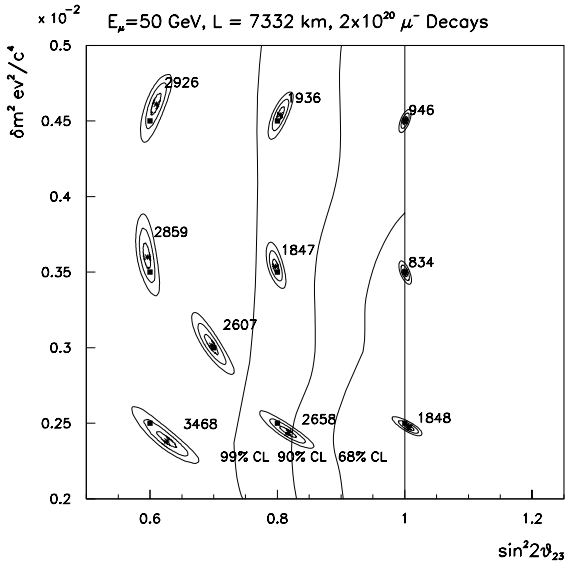

Figure 11: Fit to muon neutrino survival distribution (from (33))for $E_\mu = 50$ GeV and $L = 7332$ km for 10 pairs of $\sin^2 2\theta$, Δm^2 values. For each fit, the 1σ, 2σ and 3σ contours are shown. The generated points are indicated by the dark rectangles and the fitted values by stars. The SuperK 68%, 90%, and 95% confidence levels are superimposed. Each point is labelled by the predicted number of signal events for that point.

measurement.

Fig. 11 from reference (33) shows a fit to the atmospheric parameters for $E_\mu = 50$GeV with $L = 7332$ km, but with only one year or 2×10^{20} useful μ^- decays. The precision on $\sin^2 2\theta_{23}$ is 0.0064 and the precision on Δm^2_{32} is about $5 \times 10^{-5} eV^2$. All the other parameters are fixed and assumed to be known with perfect precision, which is reasonable given that they contribute so little to the disappearance probability. See reference (88, 73, 83) for further discussion.

6.2 Evidence for or Constraints on θ_{13}

If the solar solution is other than LMA, θ_{13} can be measured very precisely, since the correlations between Δ and θ_{13} can be ignored. Figure 12(left) from reference (30), shows the exclusion plot at 90% CL for θ_{13} in this case as a function of Δm^2_{23}, including background errors and detection efficiencies. Note that the sensitivity is best at an intermediate distance, say 3500 km , since at "low" distances the backgrounds are too problematic, and at higher distances the event rate is too small. The sensitivity to θ_{13} is in the vicinity of 0.1°, a factor 100 (in angle!) with respect to the CHOOZ limit and at least a factor 30 with respect to the projected sensitivity of JHF.

If the solar solution is LMA, however, then the value of θ_{13} for which one would still see $\nu_e \rightarrow \nu_\mu$ is a strong function of the solar mass splitting. Figure 12(right) from reference (91) shows how large $\sin^2 2\theta_{13}$ must be in order to simply measure 10 events corresponding to $\nu_e \rightarrow \nu_\mu$ transitions as a function of Δm^2_{21}. A minimum of $4\,GeV$ was required for the muons, to remove backgrounds. The different curves are for neutrino factories from 20 to 50 GeV, at a baseline of 2900km, assuming Δm^2_{23} is $3.5 \times 10^{-3} eV^2$. Note that if in fact θ_{13} is very small, a neutrino factory could be seeing evidence for and providing confirmation of the solar mass splitting. If Δm^2_{12} is very large, then measuring a non-zero value of θ_{13} will require the subtraction of the "background" from the other mass splitting scale. This will be a fortunate "background" to have to subtract, however, since this background may be due to the CP-violating terms!

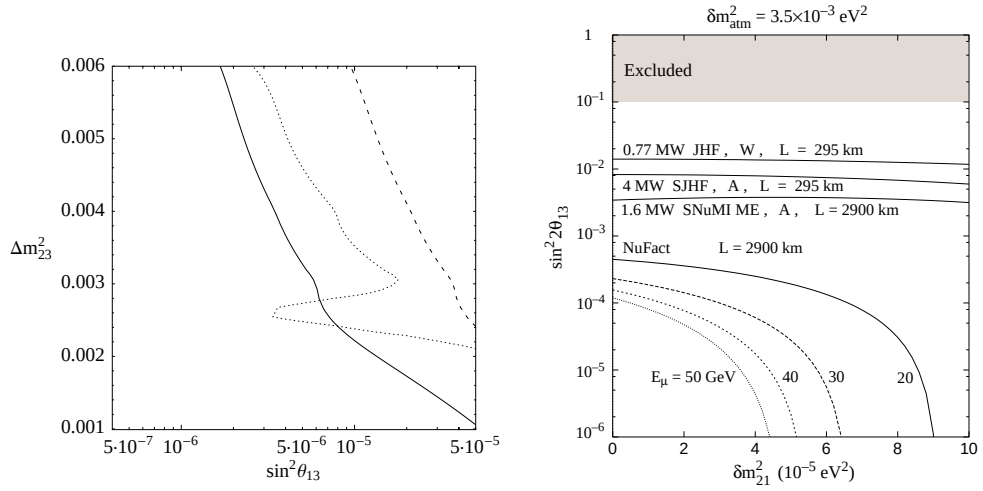

Figure 12: *left:* Asymptotic 90% confidence level sensitivity to $\sin^2\theta_{13}$ as a function of Δm^2_{23} at 90% CL for $L = 732$ km (dashed lines), 3500 km (solid lines) and 7332 km (dotted lines), assuming non LMA solution for the solar oscillation. The non-trivial shape for the dotted line occurs because you are near the peak of the oscillation, for a $50\,GeV$ neutrino factory. The sensitivity includes realistic background errors and detection efficiencies. *right:* How large $\sin^2 2\theta_{13}$ must be as a function of Δm^2_{12} to see 10 events (with a 4 GeV muon momentum cut to remove backgrounds) for different solar mass splittings and different neutrino storage ring energies, for a baseline of 2800km.

6.3 Neutrino Mass Pattern and the Effect of CP

Next we consider the determination of the neutrino mass pattern. This can be determined by comparing the wrong-sign muon rates and/or the associated CC event energy distributions when positive and then negative muons are stored in the ring. In fact, one will do exactly the same thing to measure the CP odd asymmetry.

Let us start with a simple approach and assume that θ_{13} has already been

roughly measured, following (88). Define the ratio:

$$R_{e\mu} = \frac{N(\bar{\nu}_e \to \bar{\nu}_\mu)}{N(\nu_e \to \nu_\mu)} \tag{26}$$

$R_{e\mu}$ is just the ratio of wrong-sign muon rates when respectively negative and positive muons are stored in the neutrino factory. Fig. 13 shows the predictions for $R_{e\mu}$ versus the baseline L for 10^{21} useful muon decays of both charges, a 50 kton detector, and $\Delta m^2_{32} = 3.5 \times 10^{-3}$ eV^2, $\theta_{23} = 45^\circ$ and $\sin^2 2\theta_{13} = 0.004$. The error bars correspond to statistical uncertainties for full statistics. Results for phases $\delta = 0^\circ$, $\delta = 90^\circ$, and $\delta = -90^\circ$ are shown in each case, for both positive and negative values of Δm^2_{32}. Notice the strong dependence on the sign of Δm^2_{32}, due to different matter effects for neutrinos and antineutrinos (provided that $L \succeq 2000$km) and the smaller dependence on the CP-violating phase. Reference (93) shows that with only 10^{20} useful μ^+ and μ^- decays and a 50kton MINOS-like detector (with a minimum muon momentum cut of 4GeV on the muons to remove backgrounds) one can identify the sign of the largest mass splitting at baselines above about 2000km, provided that $\sin^2 2\theta_{13}$ is larger than about 0.001 to 0.002, depending on the neutrino mass hierarchy itself. See (77, 34, 35) for further discussion.

6.4 CP Violation: Discovery and Precision

By looking carefully at figure 13, one can see that at baselines of a few thousand kilometers one might be able to detect the presence of maximal CP violation (i.e. discriminate between $\delta = 0$ and $\delta = 90^\circ$). In this section we describe the extraction of both θ_{13} and δ simultaneously. One might think "two measurements, two unknowns, what's the issue?". However, the way that these two variables are correlated depends on the baseline at which you measure the oscillation probabilities,

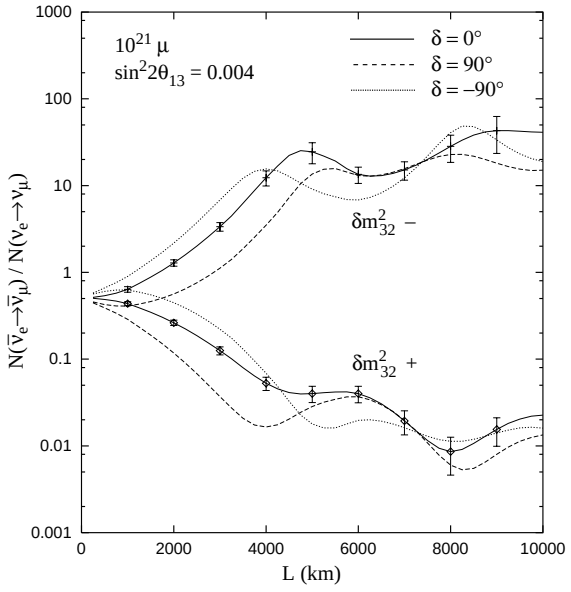

Figure 13: The ratio R of $\bar{\nu}_e \to \bar{\nu}_\mu$ to $\nu_e \to \nu_\mu$ event rates at a 20 GeV neutrino factory for $\Delta = 0, \pm\pi/2$, corresponding to the cases of no CP and maximal CP violation. The ratio at $L = 0$km is simply due to the difference in antineutrino and neutrino cross sections. The upper group of curves is for $\Delta m^2_{32} < 0$, the lower group is for $\Delta m^2_{32} > 0$, and the statistical errors correspond to 10^{21} muon decays of each sign and a 50 kton detector. The oscillation parameters correspond to the LAM solar solution with $|\Delta m^2_{32}| = 3.5 \times 10^{-3}$ eV^2 and $\sin^2 2\theta_{13} = 0.004$.

and also the sizes of the various matrix elements and mass splittings. Although we will describe here two analyses which consider a steel-scintillator sandwich detector and a 50GeV neutrino factory (30, 85), reference (94) describes an analysis for a liquid argon TPC with a magnetic field operating at a lower energy neutrino factory (but higher muon currents in the ring). There has been much written generally about this measurement. The interested reader should also see (95).

Long ago, Equation 13 gaves the transition probability of $\nu_e \to \nu_\mu$ in vacuum.

In the presence of matter, to first order one simply substitutes the mass difference Δm^2_{23} by an "effective mass difference" and the mixing angle $sin^2 2\theta_{13}$ by an "effective mixing angle". Keeping the second order terms as well as the first, the oscillation probabilities in matter can be expressed as follows (30):

$$\begin{aligned} P_{\nu_e\nu_\mu(\bar{\nu}_e\bar{\nu}_\mu)} &= s^2_{23}\sin^2 2\theta_{13}\left(\frac{\Delta_{13}}{\tilde{B}_\mp}\right)^2 \sin^2\left(\frac{\tilde{B}_\mp L}{2}\right) + c^2_{23}\sin^2 2\theta_{12}\left(\frac{\Delta_{12}}{A}\right)^2 \sin^2\left(\frac{A\,L}{2}\right) \\ &+ \tilde{J}\,\frac{\Delta_{12}}{A}\,\frac{\Delta_{13}}{\tilde{B}_\mp}\sin\left(\frac{AL}{2}\right)\sin\left(\frac{\tilde{B}_\mp L}{2}\right)\cos\left(\pm\delta - \frac{\Delta_{13}\,L}{2}\right), \end{aligned} \tag{27}$$

where L is the baseline, $\Delta_{ij} \equiv \frac{2.534\Delta m^2_{ij}}{E_\nu}$,, $\tilde{B}_\mp \equiv |A \mp \Delta_{13}|$ and A the matter parameter, related to the electron density in the earth (as described in section 2).

This can be expanded assuming θ_{13} is small, to give:

$$P_{\nu_e\nu_\mu(\bar{\nu}_e\bar{\nu}_\mu)} = X_\pm\theta^2_{13} + Y_\pm\theta_{13}\cos\left(\pm\delta - \frac{\Delta_{13}\,L}{2}\right) + P^{sol}, \tag{28}$$

where X, Y and P^{sol} are independent of θ_{13} and δ. The three terms can be considered as an atmospheric term $P^{atm}_{\nu(\bar{\nu})}$, a solar term, P^{sol} and an interference term, $P^{inter}_{\nu(\bar{\nu})}$. It is easy to show that

$$|P^{inter}_{\nu(\bar{\nu})}| \leq P^{atm}_{\nu(\bar{\nu})} + P^{sol}, \tag{29}$$

implying two very different regimes. When θ_{13} is relatively large or Δm^2_{12} small, the probability is dominated by the atmospheric term, since $P^{atm}_{\nu(\bar{\nu})} \gg P^{sol}$. We refer to this situation as the atmospheric regime. Conversely, when θ_{13} is very small (below 1° or so) or Δ_{12} is large, the solar term dominates $P^{sol} \gg P^{atm}_{\nu(\bar{\nu})}$. This is the solar regime, where matter effects are not important since one is not at all near the resonance condition for Δ^2_{12}, in other words, $\frac{2E_\nu A}{\Delta m^2_{12}}$ far from unity.

CP violation will only arise in the interference term, because of the $^\pm$ in front of the phase δ. The $\pm$ in front of the other terms are due to matter effects, and

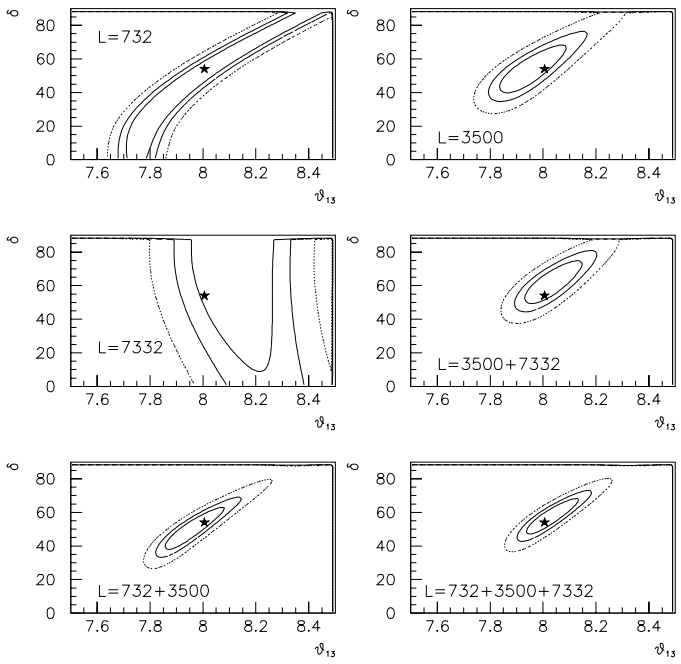

Figure 14: Simultaneous fit of θ_{13} and δ, for full statistics and taking into account background errors and detection efficiencies (from (30)).

not to any intrinsic phase in the mixing matrix. The interference term is linearly suppressed by the two small parameters: Δm^2_{12} and θ_{13}.

In the atmospheric regime the leading term, P^{atm}, does not depend on Δm^2_{12}, while it is quadratically dependent on θ_{13}. *Thus, the sensitivity to CP violation decreases linearly with* Δm^2_{12} *while it is rather stable as* θ_{13} *decreases.* This assumption breaks down as θ_{13} gets so small that the parameters are in the solar regime. In the solar regime the role of both parameters is interchanged and so *the sensitivity to CP violation decreases linearly with* θ_{13}*, but it remains rather flat with* Δm^2_{12}.

The first thing to consider is the simultaneous measurement of θ_{13} and δ, assuming fixed values of the solar and atmospheric parameters: $\Delta m^2_{23} = 2.8 \times$

$10^{-3}eV^2$, $\theta_{23} = 45°$, and LMA. Fig. 14 (from (30)) shows the one, two, and three standard deviation contours for a simultaneous fit of θ_{13} and δ for several different baselines, taking into account detector backgrounds and efficiencies, for the input values $\delta = 50°$ and $\theta_{13} = 8°$. At very short baselines, there is too much correlation between θ_{13} and δ to measure δ, and at the very long baseline there is essentially no sensitivity to δ. At the intermediate baseline of 3500 km, the two parameters can be disentangled and measured. Combining the results for 3500 km with that for any one of the other distances improves the fit, but not dramatically.

However, this is not the end of the story. Although the previous figure is illustrative, we would like to understand how the CP sensivity changes as a function of all the currently unknown parameters: δ, θ_{13}, and even Δm^2_{12}, within the LMA solution. In particular, the full range of δ should be considered, not just $0 < \delta < 90°$. Reference (85) shows how this extended range can be covered, after the suggestion (96) that the CP phase can be determined only up to a sign. It turns out that some regions of parameter space have degenerate solutions for the true parameters $(\bar{\theta_{13}}, \bar{\delta})$, that is: two different sets of values of (θ_{13}, δ) may exist which would give the same set of neutrino-antineutrino transition probabilities.

Figure 15 shows the allowed regions for θ_{13} and δ for four values of θ_{13}: two in the atmospheric region and two in the solar region ($\theta_{13} = 8, 2, 0.2, 0.6°$), and for several values of both negative and positive δ. Note that degeracies at one baseline persist in all four cases. Detector efficiencies and backgrounds have been included. Fits are presented only for $\Delta m^2_{23} > 0$. The opposite case gives better results, since for $\Delta m^2_{23} < 0$, the statistics for the signals of positive and negative wrong–sign muons are closer (so that the difference is more neatly seen).

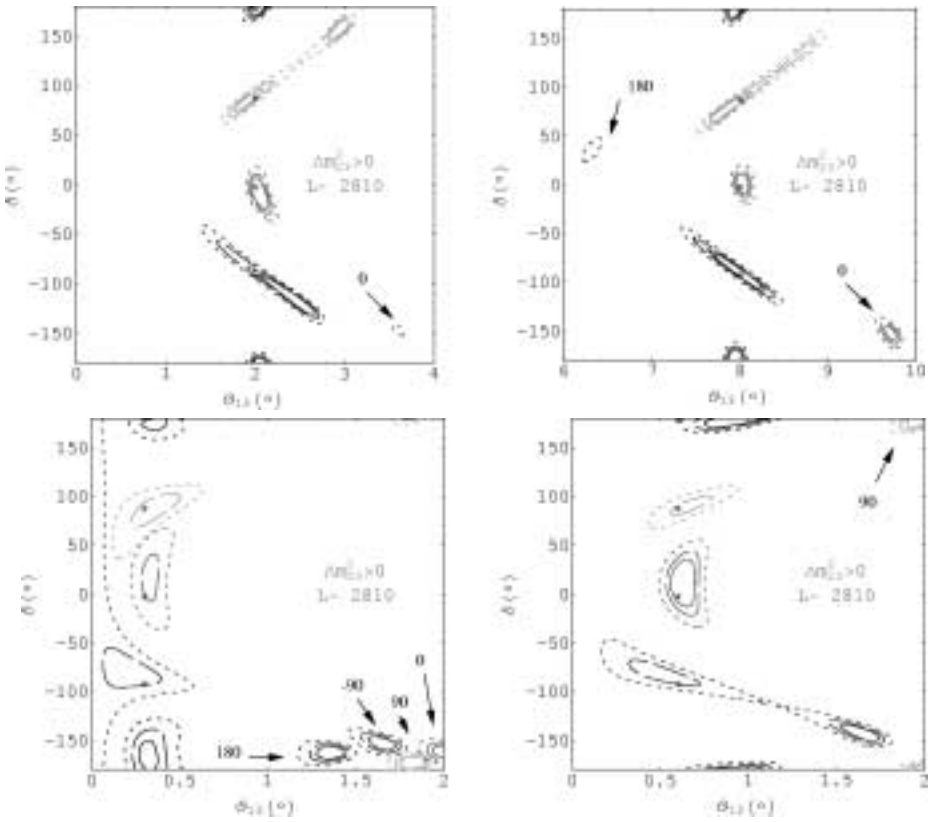

Figure 15: *Simultaneous fits of δ and θ_{13} at $L = 2810$ km for different input values (indicated by the stars) of $\bar{\delta} = -90°, 0°, 90°, 180°$ and $\bar{\theta}_{13} = 8, 2, 0.2, 0.6°$. The value of $\bar{\delta}$ for the degenerate solutions is also indicated.*

This is because matter effects enhance $P_{\bar{\nu}_e\bar{\nu}_\mu}$ instead of $P_{\nu_e\nu_\mu}$ compensating to a large extent the difference between the neutrino and antineutrino cross sections: $\sigma_\nu \simeq 2\sigma_{\bar{\nu}}$. All the results shown below correspond to the following parameter values: $\Delta m^2_{12} = 10^{-4}$ eV^2, $\Delta m^2_{23} = 3 \times 10^{-3}$ eV^2 and $\theta_{12} = \theta_{23} = 45°$.

In order to get the best precision on δ and to resolve any degeracies that are likely to arise, one would ideally like to combine two very different baseline measurements. By designing the storage ring in a bow-tie shape as shown in

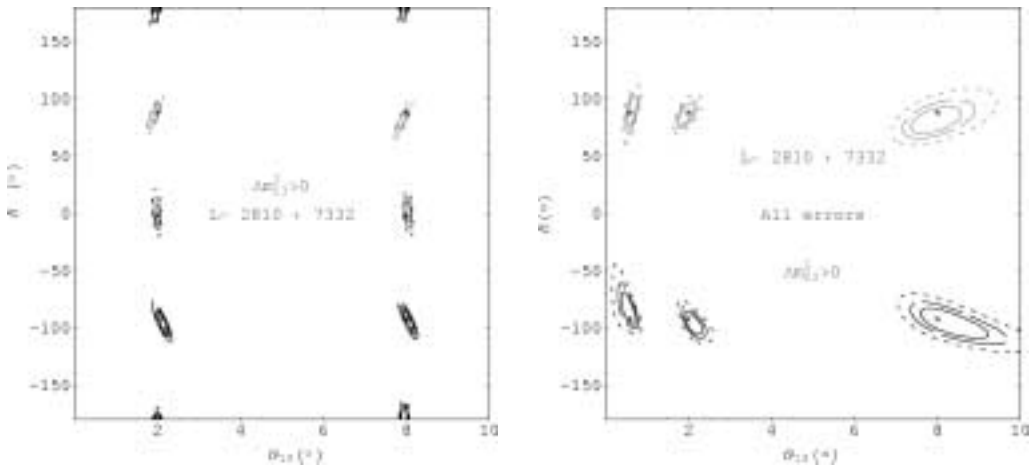

Figure 16: *Simultaneous fits of* δ *and* θ_{13} *at a combination of baselines,* $L = 2810+7332$ *km. The left plot is without and the right plot is with all uncertainties combined. The input parameter values for* $\bar{\theta}_{13}$ *range from* 0.6° *to* 8°.

Figure 7, this could be achieved. Figure 16(left) shows the result of combining the intermediate baseline with a long ($7332km$) baseline. One can see that the two-fold degeneracy disappears. The conclusion is that one needs to combine the intermediate distance with another, the far one being preferable from the point of view of degeneracies.

There is one more step to take. One must propagate all the possible errors on the parameters in the fit. Of course the solar mass splitting will not be known precisely, but rather to several per cent, and also the electron density in the earth is not known precisely, again only to a per cent or so. Although the contour lines shown in Figure 16(right) are larger than those on the left, the degeneracies noted earlier are still removed with the combination of baselines.

It has been argued (86) that in the limit of perfect energy resolution, the above degeneracies can be solved using the energy spectra. While this is certainly true in principle, the variations in energy spectra are largest at low energies, where

the acceptance is smallest due to the cuts to suppress backgrounds. Also, the detector energy resolution at low energies may also smear out what few events pass the cuts. For low energy analyses one would need at least a very different detector, for example a liquid argon TPC (94), but then achieving a large enough mass with a magnetic field would become the major challenge.

6.5 Limits of Sensitivity to CP Violation

We have shown in this section how a neutrino factory could not only discriminate between zero and maximal CP violation over a wide region of the allowed parameter space, but also how if δ is large enough, one can begin to consider measurements of delta to several degrees. The remaining task is to define for how much of the LMA range can one discriminate between maximal and 0 CP violation? This is illustrated in Figure 17. Assuming the combination of baselines, $L = 2810 + 7332$ km, the line corresponds to the minimum value of Δm^2_{12} at which the 99%CL error on the phase reaches 90° degrees, and is thus indistinguishable from 0° or 180° (i.e. no CP violation). The error on the phase is computed by taking the longest vertical size (upwards or downwards, whichever is longest) of the 99%CL contour from 90°. All errors on the parameters have been included. With this definition, there is sensitivity to CP violation for $\theta_{13} >$ few tenths of a degree and $\Delta m^2_{12} > 3 \times 10^{-5}$ eV^2.

Although some upgraded conventional beam studies have indicated a possibility of measuring delta to be non-zero in a much smaller region of parameter space (98), because one has only one baseline and one energy it will be very hard to resolve the degeneracies that are likely to occur, which would preclude a precision measurement of delta. In order to get to the bottom of what is causing leptons

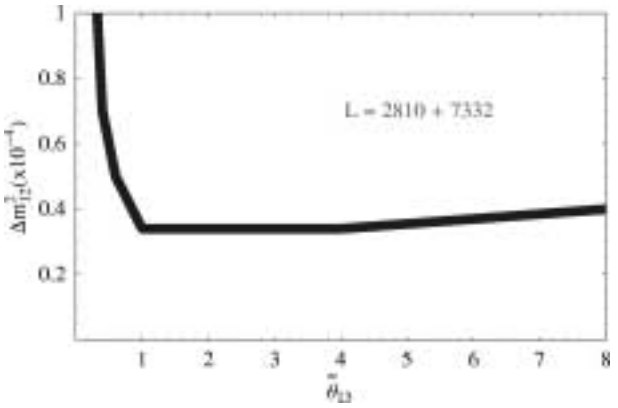

Figure 17: *Sensitivity reach for CP violation as defined in the text on the plane* $(\Delta m^2_{12}, \bar{\theta}_{13})$ *for the combination of baselines L = 2810 and 7332 km. All errors are included.*

and quarks both to mix, what is causing the world we inhabit to be quarks and not antiquarks, we would like to do much more than determine that delta is non-zero.

7 NON-OSCILLATION PHYSICS AT A NEUTRINO FACTORY

As we have just described, the high fluxes achievable at a neutrino factory would allow unprecedented measurements of the oscillation parameters at one or more far detectors. However, the increase of flux at a near detector means that still other breakthoughs can be made in complimentary areas of neutrino physics. Neutrinos have a long history of providing fundamental measurements in other branches of particle physics. They have been used as clean probes of the nucleon, and have allowed the measurements of the coupling constants of both the strong and weak forces. In order to get enough statistics to make precise measurements using neutrinos, however, extremely massive and hence rather coarse detectors were used. With a neutrino factory this would no longer have to be the case.

Table 4: Charged current muon-neutrino scattering rates in a 50cm radius target located near a muon storage ring. Rates are per 10^{20} muon decays. The detector is located $(1 \times E_\mu$, GeV)meters away from the ring to assure that primary muons have ranged out in shielding upstream of the detector.

Machine	Target	Thickness,cm	Events
50 GeV neutrino factory	Liquid H_2	100	12.1M
	Liquid D_2	100	29.0M
	solid HD	50	9.3M
	C	5.3	20.7M
	Si	6.3	25.4M
	Fe	2.3	31.6M
	Sn	3.1	39.1M
	W	1.3	44.3M
	Pb	2.4	46.5M
CCFR/NuTeV	Fe	600	$\sim$ 2M

It is rare (if not unprecedented) in experimental physics that one can get such an enormous increase in flux in just one step. Table 4 shows the event rates for detectors of various lengths of materials situated 50 m downstream of the straight section of a 50 GeV neutrino factory, operating at 10^{20} muon decays per year. These rates are compared to the event rates for recent Fermilab high-energy neutrino experiments using a conventional beam (CCFR/NuTeV): for detectors that are 100 times thinner, one can still have event rates 10 times larger (27).

The possibility of thin targets implies that a fully-active target can be used, and experiments would still get impressive statistics. Furthermore, although we

think of the deep inelastic scattering cross section as small, one can make precise measurements of use still rarer neutrino interactions (neutrino-electron scattering, for example) to get to fundamental parameters of the Standard Model. Finally, this would also be a laboratory for searches for rare processes, since again the neutrino fluxes are well-understood, and come in only two flavors. Reports which quantitatively examine these new experiments in detail can be found in references (99), (100) and (101). Here we describe only a few illustrative examples to show how different the field of "short baseline" neutrino measurements can look from how we think of it today.

7.1 Electroweak Physics

A precision measurement of the weak mixing angle, $\sin^2\theta_W$, can be achieved at a neutrino factory by measuring the scattering of neutrinos off electrons instead of off quarks. One needs a fine-grained detector to correctly isolate neutrino-electron rather than neutrino-nucleon scattering. However, because the target is an electron and not a nucleus, there are far fewer theoretical uncertainties. The challenge with this measurement is to get enough extremely fine-grained detector to do the measurement, since the cross section for neutrino-electron scattering is a factor of 2×10^4 smaller than the total cross section for deeply inelastic scattering. Liquid Argon detectors would be ideal for this measurement (99), and even one ton could provide an improvement of over an order of magnitude over the current best measurement of this parameter (102).

7.2 Neutrino Deeply Inelastic Scattering

Neutrinos have also been used historically to measure the momentum distributions of quarks inside the proton and neutron. The reason this works is the following: when neutrinos scatter off quarks, the total spin of the system is 0, and so the resulting muon direction in the center of mass is isotropic. However, when neutrinos scatter off antiquarks, the total spin of the system is 1, and so there is a very different angular distribution. From looking at Figure 1, one can see that neutrinos can have charged current scatters off $d, \bar{u}$ and $\bar{s}$ quarks, while for antineutrinos it is off $u, \bar{d}$, and s quarks. So, by measuring the kinematic distributions of these interactions for neutrinos and antineutrinos, one can take advantage of the angular dependence to extract the momentum distributions of partons in the nucleon. Specifically, if one had a pure hydrogen target, one could separate $u+\bar{d}$ quark distributions from $d+\bar{u}$ quark distributions by running neutrinos and antineutrinos separately, and then separate the quark from antiquark distributions by fits of angular distributions. However, except for liquid hydrogen bubble chamber experiments which were not very massive, contemporary experiments had heavy isoscalar targets. This means one could at best extract the sum $u + \bar{u} + d + \bar{d}$ quark distribution and the "valence quark sum", or $u - \bar{u} + d - \bar{d}$. Furthermore, one had to invoke isospin symmetry and assume that the u quark distribution in the proton is the same as the d quark distribution in the neutron.

At a neutrino factory, however, one could use liquid hydrogen or deuterium targets and still get very good statistics, as shown in Table 4. This would enable a measurement of unprecedented precision of the quark distributions in the proton and neutron separately! In addition to the high statistics, one would benefit from the fact that the neutrino source is much better known than for conven-

tional beams. Thus, it should be possible to keep the systematic errors on these measurements much lower than in previous experiments.

Finally, one can use targets of polarized materials, thereby measuring the spin components of the nucleon, quark by quark. Charged lepton scattering has been done on polarized targets, and it can be shown that at a neutrino factory even these targets (butanol, or HD) could give enough statistics to make percent or better measurements of the parton spin distributions (100),(106) (107).

7.3 Charm Production

While charm was discussed earlier as a background to wrong-sign muon searches at a neutrino factory, the same process is a signal for a near detector (see Figure 1, bottom), where the signature is two oppositely-charged muons. When a charmed meson is created, 10% of the time it will decay to a muon, and that muon has the opposite charge of the muon created by the charged-current interaction.

Even with a coarse detector, neutrino-charm production has been used in the past to measure the strange sea in the nucleon (108). Given the statistics expected, one could use this process to finally measure separately the strange and anti-strange seas in the proton and in the neutron. If one has a polarized target and sufficient statistics, one could actually extract the contribution of the strange quark to the nucleon spin. Because of the heavy mass of the charm quark, these experiments gain dramatically in statistics as the stored muon energy increases. A 50 GeV ring that produced 10^{10} charged current deep inelastic scattering events (say on a 1 ton target) would also make 4×10^8 charmed hadrons above 4GeV (101).

With a fine-grained detector, one could study the decays of the produced

charmed hadrons. For example, $D\bar{D}$ mixing would result in a signal of two same-charged muons, instead of two oppositely-charged muons. Although pions and kaons produced in the hadronic shower can also decay to a wrong-signed muon, they are more likely to interact before decaying in detectors we expect to use, whereas the charmed hadron decays quickly. So if one has a detector which can discriminate even roughly (for example, on the order of mm) the distance between the secondary and primary muon vertex, it would be straightforward to isolate the sample.

Finally, if the detector were fine grained enough, one could also study diffractive charm production, as suggested in reference (109).

7.4 Exotic Processes

Because of the large and well-understood flux of neutrinos passing through a near detector, one can look much more powerfully for exotic processes. In fact this may be the area where the most surprising results will be made at a neutrino factory– if truth be told, the motivation for the original Kamiokande experiment was *not* a search for neutrino oscillations, but a search for proton decay! One example of an exotic process one can look for at a neutrino factory is $\bar{\nu}_\mu e^- \to \mu^- \bar{\nu}_e$. Such an interaction is sensitive to new physics, since certainly no standard model process could produce this. With a 10 ton detector one can do searches which have three to four orders of magnitude more sensitivity than current limits in even a 20 GeV muon storage ring (99). Because of the very clean signature (very low transverse momentum wrong charge muon) the challenge of keeping the background at an acceptable level hopefully would not be too daunting in an appropriate detector, such as a liquid argon TPC with a magnetic field.

8 CONCLUSIONS

Neutrino physics, a ∼70year-old field, is going, not for the first time, through a period of intense experimentation and discovery. Neutrino oscillations seem the most plausible explanation to the solar and atmospheric "anomalies". The striking conclusion is that neutrinos mix, and therefore have mass.

Much remains to be learned. If the LSND signal is due to oscillations, there is still another mass splitting (and therefore at least one more massive neutrino!). This could open the door to exotic combinations of active and sterile neutrinos. The LSND signature must be confirmed or refuted. We do not know yet which solar solution has been chosen by Nature. Out of the six neutrino mixing matrix parameters, we know only roughly what two of them are $(\Delta m^2_{atm}, \theta_{23})$. Two others $(\Delta m^2_{12}, \theta_{12})$ can have still wildly different solutions, and we know next to nothing about the other two (only that θ_{13} must be smaller than about 10°). Furthermore, we cannot even say if the neutrino mass pattern follows that of the charged fermions!

The next several years of expermients will substantially advance our knowledge. MiniBooNE will confirm or refute the the LSND anomaly. KamLAND will establish whether or not the solar solution is LMA, and if so measure the solar parameters to within a few percent. Long baseline experiments (MINOS, OPERA, ICARUS) will measure the atmospheric parameters to about 10 %.

At the end of this decade, however, we will be far from done. One way to take that next step is to make even more intense conventional beams. The next generation of neutrino oscillation experiments, spearheaded by the JHF-Kamioka project, may be operational. Because the backgrounds are so high, however, for a given factor improvement, one must increase the product of detector mass and the

number of neutrinos produced by that factor squared! The second phase of the JHF-Kamioka project upgrades the proton source which supplies the neutrinos by a factor of ~ 5, and the detector mass by a factor of ~ 20 over the first phase. The first phase of JHF-Kamioka project may constrain the atmospheric parameters to precisions of a few percent, and observe $\nu_e \to \nu_\mu$ oscillations or set a stringent limit, $\theta_{13} \preceq 1 - 3^\circ$. The second phase may have a chance to observe a CP-violation in the lepton sector, if Nature is extremely kind.

The question remains: when the challenges of making a stored beam of muons can be met, will there still be oscillation measurements left to do?

The answer is, we believe, a very firm yes. Why? Because our knowledge of the leptonic mixing matrix will still be far from complete, and far from precise. Furtheremore, no other facility can provide the means for a break-through.

What will we still want to know? If θ_{13} is not known, we will want to measure it. We will have no idea how small this quantity is, and no reason to assume it is zero. If $\nu_\mu \to \nu_e$ transitions have not been observed by the next round of intense conventional neutrino beams, the neutrino factory can expand the reach on θ_{13} by at least another order of magnitude if not more. Even if θ_{13} is known, it is unlikely that we will know the neutrino mass pattern.

Finally, we come to the Holy Grail of neutrino oscillation physics, the observation of a CP-odd phase. We have seen in the previous sections that this is a most difficult task. The CP-violating asymmetries are small and the existence of degenerate solutions call for multi-baseline, extremely precise experiments.

Why don't we just make make more and more powerful conventional beams and bigger and bigger detectors? There are problems here that no amount of money can solve. A conventional beam, no matter what its intensity, has an intrinsic

background to the $\nu_\mu \to \nu_e$ oscillation search of at least around 0.5%. This background must be subtracted from any potential signal, and as a consequence, the sensitivity of a conventional beam experiment to an appearance channel does not scale linearly, but with the square root of the the number of events. The systematic error on the knowledge of the flux will be also at the few per cent level.

Understanding all the backgrounds as well as systematic errors will be of capital importance for any experiment that attempts to measure a CP-odd phase *and* resolve degenerate solutions. Recall that the neutrino factory offers a solution to all the above problems: clean beams with *zero* beam-related background, massive detectors where the background can be controlled to near the ppm level, extremely high statistics to measure the atmospheric parameters to exquisite precision, and precisely computable event rates that can be easily extrapolated from near-detector measurements, thus, extremely small beam systematic errors. Add to this the possibility to observe $\nu_e \to \nu_\tau$ transitions in liquid Argon TPC detectors, which, among other things can help in resolving the degeneracies. Last but not least, the neutrino factory can shoot simultaneously to two base lines. We have demonstrated that this is of extreme importance to control degeneracies; but it is also of great interest for redundant measurements (matter effects, atmospheric parameters).

In summary, we believe that both discovery and precision oscillation physics can, and indeed must be done at a neutrino factory. The implications for non-oscillation physics are also enormous, much larger than we have had the space to describe.

There remains one final detail that we feel we must underscore. We have seen

that a combination of both an intermediate and very long baseline is best to extract the most physics, something again only a muon storage ring can provide. A beam that travels 8000 kilometers from its source to meet an experimental area–most likely on a different continent–implies a new level of collaboration and cooperation among scientists that would enrich us all.

9 ACKNOWLEGEMENTS

This work was supported by the United States Department of Energy and the Spanish Ministry of Science and Technology. The authors wish to thank Jeff Appel, Jordi Burguet, Steve Geer, Kevin McFarland, Jorge Morfin, and Ana Tornero for their careful reading of this paper, as well as Pilar Hernández, Belén Gavela and Friedrich Dydak for very useful discussions during the writing process.

10 LITERATURE CITED

References

1. J.Tinlot, *A Storage Ring for 10 BeV Mu-Mesons* SLAC-5 (1962) 165; J.Tinlot and D.Green, UR-875-76 (1965).
2. T.L.Collins and S.Wojcicki, unpublished notes, 1974.
3. D.G. Kosharev, *Proposal for a decay ring to produce intense secondary particle beams at the sps*, CERN internal report CERN/ISR-DI/74-62 (1974).
4. R. Davis *et al.*, Phys. Rev. Lett. **20** (1968) 1205;
5. The last update of the SSM can be found in J.N. Bahcall, M.H. Pinsonneault, S. Basu, *Astrophys. J.* **555** (2001) 990.
6. B.T. Cleveland et al., *Astrophys. J.* **496** (1998) 505.

7. W. Hampel et al. (GALLEX Collaboration), *Phys.Lett.* **B 447** (1999) 127.

8. J.N. Abdurashitov et al. (SAGE Collaboration), *Phys. Rev.* **C 60** (1999) 055801 [astro-ph/9907113]; V. Gavrin (SAGE Collaboration), *Solar neutrino results from SAGE*, in *Neutrino 2000*, Proc. of the XIXth International Conference on Neutrino Physics and Astrophysics, 16–21 June 2000, eds. J. Law, R.W. Ollerhead, and J.J. Simpson, *Nucl. Phys. Proc. Suppl.* **B 91** (2001) 36.

9. Y. Fukuda et al., *Phys. Rev. Lett.* **81** (1998) 1158; Erratum **81** (1998) 4279; *Phys. Rev. Lett.* **82** (1999) 1810; Y. Suzuki (Super-Kamiokande Collaboration), *Solar neutrino results from Super-Kamiokande*, in *Neutrino 2000*, Proc. of the XIXth International Conference on Neutrino Physics and Astrophysics, 16–21 June 2000, eds. J. Law, R.W. Ollerhead, and J.J. Simpson, *Nucl. Phys. Proc. Suppl.* **B 91** (2001) 29; S. Fukuda et al. (Super-Kamiokande Collaboration), *Phys. Rev. Lett.* **86** (2001) 5651.

10. A.B. McDonald (SNO collaboration), *The Sudbury Neutrino Observatory project*, *Nucl. Phys. Proc. Suppl.* **B 77** (1999) 43; G.T. Ewan, W.F. Davidson, C.K. Hargrove (SNO Collaboration), *The Sudbury Neutrino Observatory—an introduction*, *Physics in Canada* **48** (1992) 112; SNO Collaboration, *The Sudbury Neutrino Observatory*, *Nucl. Instrum. Meth.* **A 449** (2000) 172.

11. Kamiokande Collaboration, S. Hatakeyama *et al.*, Phys. Rev. Lett. **81** (1998) 2016; Soudan-2 Collaboration, E. Peterson, Nucl. Phys. **B** (Proc. Suppl.) **77** (1999) 111; W. W. Allison, Phys. Lett. **B 449** (1999) 137; MACRO Collaboration, F. Ronga *et al.*, Nucl. Phys. **B** (Proc. Suppl.) **77** (1999) 117.

12. Super-Kamiokande Collaboration, Y. Fukuda *et al.*, Phys. Lett. **B 433** (1998) 9; Phys. Lett. **B 436** (1998) 33; Phys. Rev. Lett. **81** (1998) 1562; Phys. Rev.

Lett. **82** (1999) 2644; Phys. Lett. **B 467** (1999) 185; T. Kajita, Nucl. Phys. **B** (Proc. Suppl.) **77** (1999) 123.

13. B. Pontecorvo, J. Expt. Theor. Phys. **33** (1957) 549; J. Expt. Theor. Phys. **34** (1958) 247; Sov. Phys. JETP **26** (1968) 984.

14. Z. Maki, M. Nakagawa, and S. Sakata, Prog. Theor. Phys **28** (1962) 870.

15. S. Geer, Phy. Rev. **57**(1998)6989, *ibid* **59**(1999) 39903E.

16. C. Athanassopoulos, Phys. Rev. Lett. **75** 2650 (1995); Phys. Rev. Lett. **77** 3082 (1996); Phys. Rev. Lett. **81** 1774 (1998).

17. B. Armbruster *et al*, Phys.Rev.**C57** (1998) 3414.

18. $\mu^+\mu^-$ *Collider Feasibility Study*, The Muon Collider Collaboration, Fermilab-Conf-96/092, July 1996, unpublished. R. Palmer, A. Tollestrup, and A. Sessler, *Status Report of a High Luminosity Muon Collider and Future Research and Development Plans*, Proc. of the 1996 DPF / DPB Summer Study on New Directions for High-energy Physics (Snowmass 96), Snowmass, CO, 25 June - 12 July 1996. C. Ankenbrandt et al. (The Muon Collider Collaboration), Phys. Rev. ST Accel. Beams 2, 081001 (1999).

19. The latest results of the NOMAD collaboration concerning oscillations can be found in P. Astier et al. (NOMAD Collaboration), Nucl. Phys. **B611** (2001)3.

20. The latest results of the CHORUS collaboration concerning oscillations can be found in E. Eskut et al., (CHORUS Collaboration), Phys.Lett. **B497** (2001) 8.

21. A. De Rújula, M. B. Gavela, and P. Hernández, Nucl. Phys. **B547** (1999) 21.

22. C. Crisan and S. Geer, FERMILAB-TM-2101, Feb. 2000.

23. S. Geer and R. Raja, *"Workshop on Physics at the first muon collider and at the front end of a muon collider"*, AIP Conf. Proc. **435** (1998).

24. *Neutrino Factories based on muon storage rings. Proceedings, ICFA/ECFA workshop, NUFACT'99, Lyon, France, july 5-9, 1999* B. Autin, (ed.) Nucl.Instrum.Meth. **A451** (2000)1

25. *Proceedings of the muon storage ring for a Neutrino Factory. NUFACT'00, Monterey, USA, may 22-26, 2000.* S. Chattopadhyay, (ed.) Nucl. Instrum. Methods **A472** (2001) 323-666.

26. *Proceedings of the NUFACT01 workshop, Epochal Tsukuba, Japan, may 24-300, 2000.* To be published. Web page:
`http://psux1.kek.jp/ nufact01/index.html`

27. F. Dydak, *The Neutrino Factory*, Phys.Scripta **T93** (2001) 91; R. Raja et al., *The program in muon and neutrino physics: Super Beams, Cold Muon Beams, Neutrino Factory and the Muon Collider*, FERMILAB-CONF-01-226-E, Aug 2001. Contributed to APS / DPF / DPB Summer Study on the Future of Particle Physics (Snowmass 2001), Snowmass, Colorado, 30 Jun - 21 Jul 2001, hep-ex/0108041; M.B. Gavela, *Neutrino oscillation physics at a Nu Factory.* Nucl. Phys. Proc. Suppl. **100** (2001) 175; J.J. Gomez-Cadenas, *Measurement of cp violation at a Neutrino Factory.* Nucl. Phys. Proc. Suppl. **99B**; P.Hernandez, *Neutrino oscillation physics with a Neutrino Factory.* Nucl. Phys. Proc. Suppl. **81** (2000)167; O. Yasuda, *Phenomenology of neutrino oscillations at a Neutrino Factory*, Proceedings of KEK International Workshop on High Intensity Muon Sources (HIMUS 99), Tsukuba, Japan, 1-4 Dec 1999. e-Print Archive: hep-ph/0005134;

28. A thorough introduction to and review of current evidence for neutrino oscillation can be found in P.Fisher, B.Kayser,K.S.McFarland, Ann. Rev. Nucl. Part. Sci. **49** (1999) 481.

29. M. Apollonio *et al.*, hep-ex/9907037.

30. A. Cervera et al., Nucl. Phys. **B579** (2000) 17.

31. L. Wolfenstein, Phys. Rev. **D 17** (1978) 2369; Phys. Rev. **D 20** (1979) 2634; S. P. Mikheyev and A. Yu. Smirnov, Sov. J. Nucl. Phys. **42** (1986) 913.

32. R. H. Bernstein, S. J. Parke, Phys.Rev.**D44** (1991) 2069.

33. V. D. Barger, S. Geer, R. Raja and K. Whisnant, Phys. Rev. D **62** (2000) 013004

34. I. Mocioiu and R. Shrock, Phys. Rev. **D62** (2000) 053017.

35. M. Freund, M. Lindner, S. T. Petcov and A. Romanino, Nucl. Phys. **B578** (2000) 27.

36. M.Honda *et al.*, Phys. Lett. **B248** (1990) 193; M.Honda *et al.*, Phys. Rev. **D52** (1995) 4985.

37. G.Barr *et al.*, Phys. Rev. **D39** (1989) 3532; V.Agrawal, *et al.*, Phys. Rev. **D53** (1996) 1313; T.K.Gaisser and T.Stanev, Proc. 24th Int. Cosmic Ray Conf. (Rome) Vol.1 (1995) p694.

38. T. Kajita for the Super-Kamiokande Collaboration, *Study of neutrino oscillations with the atmospheric neutrino data from Super-Kamiokande*, Nucl. Phys. Proc. Suppl. **100** (2001) 107.

39. G. L. Fogli, E. Lisi, A. Maronne and G. Scioscia, Phys. Rev. **D59**, 033001 (1999); G.L. Fogli, E. Lisi, D. Montanino and G. Scioscia Phys. Rev. **D55**, 4385 (1997); A. De Rujula, M.B. Gavela, P. Hernandez, hep-ph/0001124; T.

Teshima, T. Sakai, Prog. Theor. Phys. **101**, 147 (1999); Prog. Theor. Phys. **102**, 629 (1999); hep-ph/0003038.

40. John N. Bahcall, *Neutrino Astrophysics*, Cambridge University Press, 1989.

41. Q.R. Ahmad et al., Phys. Rev. Lett. **87** (2001) 071301.

42. G. L. Fogli, E. Lisi, D. Montanino and A. Palazzo, Phys. Rev. **D62**, 013002 (2000); G.L. Fogli, E. Lisi, D. Montanino, Phys. Rev. **D54**, 2048 (1996).

43. J.N. Bahcall, M.C. Gonzalez-Garcia, C. Pena-Garay *Robust signatures of solar neutrino oscillation solutions*, hep-ph/0111150.

44. J.N. Bahcall, M.C. Gonzalez-Garcia, C. Pena-Garay *Global analysis of solar neutrino oscillations including sno cc measurement*, hep-ph/0106258, JHEP 0108:014,2001.

45. M.C. Gonzalez-Garcia, M. Maltoni, Carlos Pena-Garay, J.W.F. Valle Phys. Rev. **D63** (2001) 033005.

46. G.L. Fogli, E. Lisi, A. Marrone, hep-ph/0105139.

47. O. Yasuda, hep-ph/0006319.

48. M.C. Gonzalez-Garcia, M. Maltoni, Carlos Pena-Garay, Phys. Rev. **D64** (2001) 093001.

49. S. Fukuda *et al.* [Super–Kamiokande Collaboration], Phys. Rev. Lett. **85**, 3999 (2000).

50. D. Dooling, C. Giunti, K. Kang and C.W. Kim, Phys. Rev. D **61**, 073011 (2000).

51. A. Donini, M. B. Gavela, P. Hernandez and S. Rigolin, Nucl. Instrum. Meth. A **451** (2000) 58 [arXiv:hep-ph/9910516]. A. Kalliomaki, J. Maalampi and M. Tanimoto, Phys. Lett. B **469** (1999) 179 [arXiv:hep-ph/9909301].

A. Donini and D. Meloni, Eur. Phys. J. C **22** (2001) 179 [arXiv:hep-ph/0105089]. A. Donini and D. Meloni, arXiv:hep-ph/0107274. V.D.Barger, S.Geer,R.Raja, K.Whisnant, Phys.Rev.**D63** 033002 (2001)

52. G. Barenboim, L.Borissov, J.Lykken, A.Y.Smirnov, hep-ph/0108199.

53. S.J.Huber, Q.Shafi, Phys. Lett. **B512** 365 (2001)

54. `http://www-boone.fnal.gov/`

55. J. Busenitz *et al.,* "Proposal for US Participation in KamLAND," March 1999 (unpublished). May be downloaded from http://bfk0.lbl.gov/kamland/.

56. V. Barger, D. Marfatia, and B.P. Wood, *Phys. Lett.* **B498**, 53 (2001).

57. H. Murayama and A. Pierce, Phys. Rev. **D65** (2002) 013012.

58. A. de Gouvea, C. Pena-Garay, Phys. Rev. **D64** (2001) 113011.

59. S.H. Ahn et al., (the K2K collaboration),*Detection of Accelerator-Produced Neutrinos at a Distance of 250 km* hep-ex/0103001. S.Boyd (for K2K collaboration),*Recent Results from the K2K (KEK-to-Kamioka) Neutrino Oscillation Experiment*,Sixth International Workshop on Tau Lepton Physics, Victoria, BC, Canada, September 19, 2000. hep-ex/0011039.
See `http://neutrino.kek.jp/publications/` for further references.

60. MINOS Technical Design Report NuMI-L-337 TDR,
V. Paolone Nucl. Phys. Proc. Suppl. **100** (2001)197. S. G. Wojcicki, Nucl. Phys. Proc. Suppl. **91** (2001) 216.

61. OPERA Progress Report, LNGS-LOI 19/99,
`http://operaweb.web.cern.ch/operaweb/`

62. CLONING OF T600 MODULES TO REACH THE DESIGN SENSITIVE MASS ICARUS-TM/2001-08 LNGS-EXP 13/89

63. J. Altegoer *et al.* [NOMAD "The NOMAD experiment at the CERN SPS," Nucl. Instrum. Meth. **A404**, 96 (1998).

64. Y.Itow *et al* ,"The JHF-Kamioka Neutrino Project", *hep-ex/0106019.*

65. M. Furusaka, R. Hino, Y. Ikeda *et al.*, *"The Joint Project for High-Intensity Proton Accelerators"*, KEK Report 99-4; JAERI-Tech 99-056; JHF-99-3 (1999).

66. B. Autin, A. Blondel and J. Ellis, (ed.) *"Prospective study of muon storage rings"*, CERN 99-02, ECFA 99-197;

67. T. Anderson *et al*, (Eds: N. Holtkamp, D.A. Finley), FERMILAB-PUB-00-108-E (2000)

68. M. Goodman *et al*, (Eds: S.Ozaki, R.Palmer, M.Zisman,J.Gallardo), "Feasibility Study II of a Muon-Based Neutrino Source", BNL-52623 (2001).

69. Y. Kuno et al., *A feasibility study of a Neutrino Factory in Japan*, unpublished. Web page; `http://www-prism.kek.jp/nufactj/index.html`

70. See for example the contribution of J. Collot et al, to the proceedings of NUFACT99, (24).

71. For more details, see, for example, R.B.Palmer, C.Johnson and E.Keil,*A cost-E fective design for a Neutrino Factory*, in proceedings of NUFACT99, (24), and E.J.N.Wilson,A.M. Sessler,*Summary of scenarios working groups, ibid.*

72. See for example: T. K. Gaisser, *"Cosmic Rays and Particle Physics"*, Cambridge University Press, 1990.

73. V. D. Barger, S. Geer, R. Raja and K. Whisnant, Phys. Rev. D **62** (2000) 073002 [arXiv:hep-ph/0003184].

74. C. K. Jung, *Feasibility of a next generation underground water Cherenkov detector: UNO*, arXiv:hep-ex/0005046.

75. A. Cervera, F. Dydak and J. Gomez Cadenas, Nucl. Instrum. Meth. A **451** (2000) 123.

76. F. Arneodo *et al.* [ICARUS Collaboration], Nucl. Instrum. Meth. A **471** (2000) 272. A. Rubbia, *Status Of The Icarus Experiment*, Phys. Scripta **T93** (2001) 70.

77. A. Bueno, M. Campanelli and A. Rubbia, Nucl. Phys. **B589** (2000) 577.

78. A. Blondel, Nucl. Instrum. Meth. A **451** (2000) 131.

79. T. Ota, J. Sato, Y. Kuno, Phys.Lett.**B520** (2001) 289.

80. As propossed by the now-defunct ICANOE Collaboration; *ICANOE:A proposal for a CERN-GS long baseline and atmosferic neutrino oscillation experiment*,INFN/AE-99-17,LNGS-P21/99,CERN/SPSC 99-25,SPSC/P314; ICARUS detector module,Proceedings of the *Frontiers Detectors for Frontier Physics* I.la d Elba,Italy,May 2000;Nucl.Instr.and Meth.A 461 (2001)(special issue).

81. M. Campanelli, A. Bueno and A. Rubbia, Nucl. Instrum. Meth. A **451** (2000) 176.

82. A. Bueno, M. Campanelli, S. Navas-Concha and A. Rubbia, *On the energy and baseline optimization to study effects related to the delta-phase (CP-/T-violation) in neutrino oscillations at a neutrino factory.* arXiv:hep-ph/0112297.

83. C. Albright, et al., *Physics at a Neutrino Factory*, FERMILAB-FN-692, Aug 2000, hep-ex/0008064;

84. V. Barger, D. Marfatia and B.P. Wood, hep-ph/0011251.

85. J. Burguet-Castell, M. B. Gavela, J. J. Gomez-Cadenas, P. Hernandez and O. Mena, Nucl. Phys. B **608** (2001) 301 [arXiv:hep-ph/0103258].

86. M. Freund, P. Huber and M. Lindner, Nucl. Phys. B **615** (2001) 331 [arXiv:hep-ph/0105071].

87. S. M. Bilenky, T. Lachenmaier, W. Potzel and F. von Feilitzsch, arXiv:hep-ph/0109200; P. Aliani, V. Antonelli, M. Picariello and E. Torrente-Lujan, arXiv:hep-ph/0112101.

88. V.Barger, S.Geer, R.Raja, K.Whisnant, Phys. Rev. **D63** (2001) 033002.

89. P. Lipari, Phys. Rev. **D61** (2000) 113004.

90. J. Ellis, hep-ph/9911440.

91. V. Barger, et al. FERMILAB-FN-703 [arXiv:hep-ph/0103052], V.D. Barger, S.Geer, R.Raja, and K.Whisnant, Phys. Rev. **D63** (2001) 113011.

92. M. Campanelli, A. Bueno and A. Rubbia, Nucl. Instrum. Meth. A **451** (2000) 207.

93. V. D. Barger, S. Geer, R. Raja and K. Whisnant, Phys. Rev. B **485** (2000) 379.

94. A. Bueno, M. Campanelli, S. Navas-Concha, A. Rubbia , `hep-ph/0112297`

95. J. Arafune, M. Koike and J. Sato,
Phys. Rev. **D 56** (1997) 3093, Erratum-Ibid. **D 60** (1999) 119905;
M. Tanimoto, Prog. Theor. Phys. **97** (1997) 9091;
Phys. Lett **B 435** (1998) 373; Phys. Lett. **B 462** (1999) 115;
H. Minakata and H. Nunokawa, Phys. Lett. **B 413** (1997) 369;
Phys. Rev. **D 57** (1998) 4403;

S. M. Bilenky, C. Giunti and W. Grimus, hep-ph/9705300; Phys. Rev. **D 58** (1998) 033001. K. R. Schubert, hep-ph/9902215; J. Bernabéu, hep-ph/9904474;

H. Fritzsch and Z. -Z. Xiang, hep-ph/9909304; A. Romanino, hep-ph/9909425;

M. Koike and J. Sato, hep-ph/9909469; J. Sato, hep-ph/9910442.

96. P. Lipari, hep-ph/0102046.

97. A. Donini *et al*, Nucl.Phys. **B574** (2000) 23.

98. H. Minakata and H. Nunokawa, JHEP **0110** (2001) 001 [arXiv:hep-ph/0108085].

99. I.Y.Bigi *et al*, `hep-ph/0106177`, submitted to Physics Repots.

100. M.L.Mangano *et al*, `hep-ph/0105155` , Report of the nuDIS Working Group for the ECFA-CERN Neutrino- Factory study.

101. K.S. McFarland, Nucl. Instrum. Meth. **A451** (2000) 218;

102. G.P.Zeller, K.S.McFarland *et al*, Phys. Rev. Lett. **88**, 91802 (2002).

103. W.G. Seligman *et al.*, Phys. Rev. Lett. **79**, 1213 (1997).

104. J. P. Berge *et al.*, Z. Phys. **C49**, 187 (1991).

105. P. Annis [CHORUS Collaboration], Nucl. Instrum. Meth. **A409**, 629 (1998). M. G. van Beuzekom *et al.* [CHORUS Collaboration], Nucl. Instrum. Meth. **A427**, 587 (1999). E. Eskut *et al.* [CHORUS Collaboration], Phys. Lett. **B434**, 205 (1998).

106. R.D.Ball, D.A.Harris, K.S.McFarland `hep-ph/0009223` submitted to Phys. Rev. **D**.

107. E.Leader, J. Phys. **G 27** 2171 (2001)

108. M. Goncharov *et al*, Phys. Rev. **D64** 112006 (2001)

109. G. De Lellis, P. Migliozzi, P. Zucchelli, Phys. Lett. **B507** 7 (2001).